Design, Synthesis and Biological Evaluation of Potent Azadipeptide Nitrile Inhibitors and Activity-Based Probes as Promising Anti-Trypanosoma brucei Agents

ARTICLE *in* CHEMISTRY - A EUROPEAN JOURNAL · MAY 2012

Impact Factor: 5.73 · DOI: 10.1002/chem.201103322 · Source: PubMed

6 AUTHORS, INCLUDING:

Pengyu Yang
The Scripps Research Institute
29 PUBLICATIONS **976** CITATIONS
SEE PROFILE

Cynthia Y He
National University of Singapore
34 PUBLICATIONS **1,087** CITATIONS
SEE PROFILE

Shao Q Yao
National University of Singapore
190 PUBLICATIONS **5,043** CITATIONS
SEE PROFILE

DOI: 10.1002/chem.201103322

Design, Synthesis and Biological Evaluation of Potent Azadipeptide Nitrile Inhibitors and Activity-Based Probes as Promising Anti-*Trypanosoma brucei* Agents

Peng-Yu Yang,[a] Min Wang,[b] Lin Li,[a] Hao Wu,[a] Cynthia Y. He,*[b] and Shao Q. Yao*[a]

Abstract: *Trypanosoma cruzi* and *Trypanosoma brucei* are parasites that cause Chagas disease and African sleeping sickness, respectively. There is an urgent need for the development of new drugs against both diseases due to the lack of adequate cures and emerging drug resistance. One promising strategy for the discovery of small-molecule therapeutics against parasitic diseases has been to target the major cysteine proteases such as cruzain for *T. cruzi*, and rhodesain/TbCatB for *T. brucei*. Azadipeptide nitriles belong to a novel class of extremely potent cysteine protease inhibitors against papain-like proteases. We herein report the design, synthesis, and evaluation of a series of azanitrile-containing compounds, most of which were shown to potently inhibit both recombinant cruzain and rhodesain at low nanomolar/picomolar ranges. A strong correlation between the potency of rhodesain inhibition (i.e., target-based screening) and trypanocidal activity (i.e., whole-organism-based screening) of the compounds was observed. To facilitate detailed studies of this important class of inhibitors, selected hit compounds from our screenings were chemically converted into activity-based probes (ABPs), which were subsequently used for in situ proteome profiling and cellular localization studies to further elucidate potential cellular targets (on and off) in both the disease-relevant bloodstream form (BSF) and the insect-residing procyclic form (PCF) of *Trypanosoma brucei*. Overall, the inhibitors presented herein show great promise as a new class of anti-trypanosome agents, which possess better activities than existing drugs. The activity-based probes generated from this study could also serve as valuable tools for parasite-based proteome profiling studies, as well as bioimaging agents for studies of cellular uptake and distribution of these drug candidates. Our studies therefore provide a good starting point for further development of these azanitrile-containing compounds as potential anti-parasitic agents.

Keywords: azo compounds · click chemistry · drug discovery · high-throughput screening · proteomics · structure–activity relationships

Introduction

Chagas disease (or American trypanosomiasis) is caused by *Trypanosoma cruzi* and affects around 12 million people in Latin America, resulting in approximately 14,000 deaths per year.[1] More recently, due to immigrant carriers or infections from contaminated transfusions and organ transplants, Chagas disease has been reported in areas in which it normally does not exist.[2] Human African trypanosomiasis (HAT, sleeping sickness) is caused by tsetse fly transmitted parasites of *Trypanosoma brucei*. Over 60 million people in sub-Saharan Africa are at risk of this disease, of which there are already 50,000–70,000 confirmed cases.[3] Existing drugs used to treat these diseases are generally highly toxic and often ineffective, and drug resistance has developed in some cases (see Figure S1 in the Supporting Information).[4] With no immediate prospect of vaccines, there is an urgent need to develop new trypanocidal agents with acceptable efficacy and safety profiles. One encouraging approach to novel anti-parasitic agents is the development of small-molecule inhibitors targeting parasitic cysteine proteases such as cruzain (an essential protease for the survival of *T. cruzi*[5]), rhodesain (also known as brucipain, trypanopain) and, more recently, TbCatB (a cathepsin B-like protease) in *T. brucei*.[6] Cysteine proteases are fundamental to the metabolism of many parasites,[7] and their inhibitors have been shown to kill protozoan parasites in both culture and animal models. One such inhibitor, *N*-Mpip-Phe-Hph-VSPh (also known as K11777; Figure 1A) is currently in late-stage preclinical trials for treatment of Chagas disease.[8] K11777 was also

[a] P.-Y. Yang, Dr. L. Li, H. Wu, Prof. Dr. S. Q. Yao
Department of Chemistry
National University of Singapore
3 Science Drive 3
Singapore 117543 (Singapore)
Fax: (+65) 6779-1691
E-mail: chmyaosq@nus.edu.sg

[b] M. Wang, Dr. C. Y. He
Department of Biological Sciences
National University of Singapore
14 Science Drive 4
Singapore 117543 (Singapore)
E-mail: dbshyc@nus.edu.sg

Supporting information for this article is available on the WWW under http://dx.doi.org/10.1002/chem.201103322.

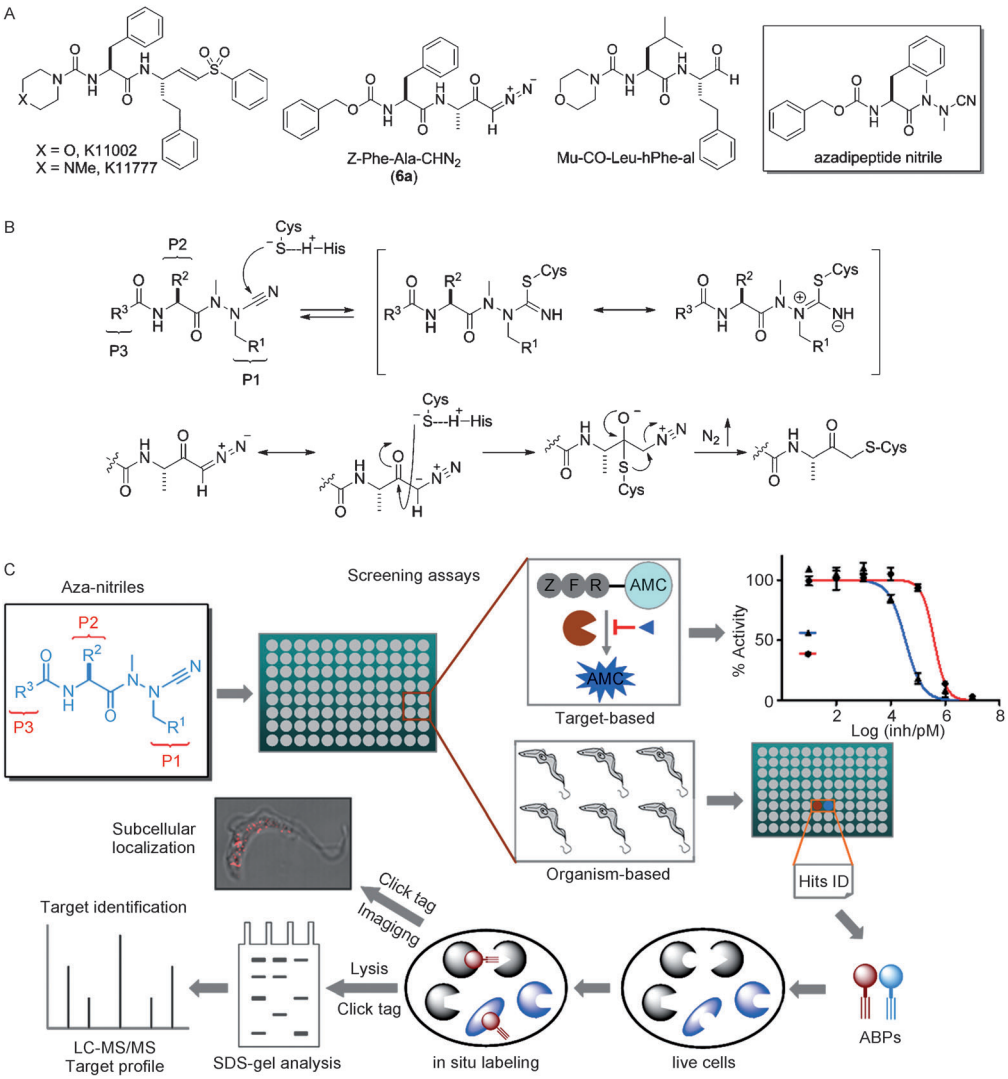

Figure 1. A) Representative structures of anti-parasitic cysteine protease inhibitors. B) Proposed inhibitory mechanism of cysteine proteases by azanitriles (top) and diazomethyl ketones (bottom). C) Overall workflow of chemical screens and characterizations of azanitriles that were screened with target-based (cruzain and rhodesain) and organism-based assays, and conversion of hit molecules into activity-based probes (ABPs). Putative identification of cellular targets (on and off) was achieved by in situ parasite-based proteome profiling. Reaction of the alkyne handle on the probe with rhodamine-azide by using click chemistry allows visualization of target proteins by SDS-PAGE gel or fluorescence microscopy. Alternatively, with biotin-azide, the probe-labeled parasite proteome could be pulled-down/LC-MS/MS for target identification.

shown to have potent in vitro and in vivo bioactivities against *T. brucei*,[9] presumably by targeting rhodesain, TbCatB, or both (the inhibitor is non selective).[10] Another cysteine protease inhibitor, Z-Phe-Ala-CHN_2 (**6a**; Figure 1 A), has also been shown to be lethal to *T. brucei* in both in vitro and in vivo studies.[11] Vinyl sulfones, tetrafluorophenoxymethyl ketones, and diazomethyl ketones, all of which contain an electrophilic "warhead" that can covalently and irreversibly inactivate cruzain as a result of nucleophilic attack by the active-site cysteine (a representative example is shown in the bottom Scheme of Figure 1 B), are also known parasiticidal agents.[12,13] Vinyl sulfones are also well-known proteasome inhibitors.[14] Previous work in developing antimalarial compounds showed that synthetic peptidyl aldehydes were potent reversible inhibitors of the cysteine protease hemoglobinases, falcipain-2 and falcipain-3.[15] One such compound, Mu-CO-Leu-hPhe-al (Figure 1 A), which exhibits strong inhibitory activity on falcipains and cultured *Plasmodium falciparum* parasites, was tested in a murine malaria model.[15] Recently, Gütschow and coworkers reported proteolytically stable azadipeptide nitriles as a novel class of cysteine protease inhibitors that form covalent but slow-releasing, reversible isothiosemicarbazide adducts with the active-site cysteine (Figure 1 B; top).[16] Using cathepsin K as an example, the authors further demonstrated that structural optimizations of azadipeptide nitriles could result in the generation of selective cathepsin inhibitors.[17] A subsequent study clearly demonstrated that azadipeptide nitriles also possessed potent antimalarial activities.[18] An organelle-specific drug delivery system using

such compounds was recently reported to directly target cathepsins in human cells.[19] In the current study, we have taken efforts to further optimize this class of inhibitors as potential agents against trypanosome parasites, with the ultimate aim of generating highly potent inhibitors that possess fewer off-targets and side effects (which are often associated with irreversible enzyme inhibitors).[20] Herein, we report the chemical synthesis and biological evaluation of a series of azanitrile-containing inhibitors, as well as some activity-based probes derived from selected compounds. By first screening these compounds against purified recombinant cruzain and rhodesain (i.e., target-based screening), we found most of them were indeed highly potent inhibitors, with IC_{50} values in the low nanomolar/picomolar ranges. Because inhibitor sensitivities are often affected by assay conditions such as pH, ionic strength, and the presence of lipids or other proteins,[21] we subsequently carried out whole-organism-based screening and quantitatively verified the potencies of some of these compounds. A good correlation between the potency of rhodesain inhibition and the trypanocidal activity of these compounds was observed. Next, by taking advantage of the covalent nature of these inhibitors, we combined the whole-organism-based screening with activity-based protein profiling (ABPP) coupled with bioorthogonal click chemistry,[22,23] and carried out comprehensive proteome profiling experiments against selected hit compounds in an effort to identify both on- and off-targets, which provided invaluable insights into the mode-of-action and further optimizations.[21] Finally, fluorescence imaging experiments with the probes provided further information on the compound's cellular uptake and sub-cellular distribution (Figure 1C).

Results and Discussion

Design and synthesis of azadipeptide nitriles: Isoelectronic replacement of the $C_\alpha H$ group by a nitrogen atom to yield azapeptides is a common structural modification in the chemistry of peptides and peptidomimetics.[24] This structural modification was first applied to the P_1 position of peptide nitriles in 2008.[16] The resulting azadipeptide nitriles were characterized as highly potent inhibitors of cysteine cathepsins (i.e., cathepsins L, S, and K). These compounds possess a methylated P_2–P_1 peptide bond, which accounts for their stability towards proteolytic cleavage. Such azadipeptide nitriles also showed time-dependent inhibition, and the reversible formation of adducts with the active site cysteine was proposed (Figure 1B; bottom). The strategy we undertook in the current work built on these initial results to further demonstrate potent inhibition of cruzain and rhodesain by azanitrile-containing compounds, because both enzymes are structurally homologous to cathepsin L. Previous studies showed that cruzain was effectively inhibited by vinyl sulfones bearing Leu or Phe residues at the P_2 position (for example, K11777/K11002). However, the P_1 and P_3 groups were considered to be less important, due to their solvent exposure, as seen in the protein structure.[25] In other words, the urea group at the P_3 position in K11777/K11002 did not actively participate in binding interactions with the enzyme; therefore, this moiety could be replaced by a carbamate group, or an amide group.[26] The designed library was based on the scaffold presented in Scheme 1, in which R^3 was either 2,3-dihydro-1,4-benzodioxin-6-yl (resulting in an amide group at the P_3 position) or carbamoyl, that is, *t*BuO or BnO, as previously reported.[16] The R^2 moiety could be either phenyl, isopropyl, or isobutyl, so that the amino acid at the P_2 position was either Phe, Val, or Leu, respectively. The highest variability was introduced at the P_1 position with five different groups (Me, Bn, CH_2Bn, CH_2CH_2Bn, or *n*-butyl), thereby enabling a systematic evaluation of the structure–activity relationship (SAR) between members of this library and their inhibitory action against cruzain/rhodesain. In this context, it is noteworthy that the structural diversity of this library can be easily increased by further variations at the P_1, P_2, and P_3 positions using the same chemistry developed herein. As shown in Scheme 1, the synthesis of our library was accomplished by modifications of previously reported procedures for the preparation of **3b** and its derivatives.[16] Starting from commercially available Boc-protected amino acids, we prepared the corresponding benzyl esters and then removed the amine protecting group by using standard methods, giving **7a–c**. The products were then coupled with 1,4-benzodioxane-6-carboxylic acid to give **8a–c**. Subsequent deprotection was carried out hydrogenolytically to give **9a–c**, which, upon coupling with methylhydrazine, gave the corresponding hydrazones **10a–c**. These compounds were subjected to reductive amination using a range of aldehydes (e.g., R^2CHO) together with dimethylamine–borane complex as the reducing regent, giving the corresponding N^1-methyl-N^2-alkylhydrazides (**12a–o**). Upon treatment with cyanogen bromide under basic conditions, the desired azanitriles **1a–o** were obtained. For the preparation of analogue **2**, the key intermediate, N^1-methyl-N^2-alkylhydrazide **15**, was prepared by using sodium cyanoborohydride in the presence of acetic acid,[27] instead of dimethylamine–borane complex. Azanitriles **3a–e** were similarly prepared, as shown in Scheme 1, from Cbz-protected phenylalanine. For the synthesis of aldehyde inhibitor **4** (an analogue of Mu-CO-Phe-hPhe-al;[15] Figure 1A), initial attempts involving oxidation of the corresponding primary alcohol with Dess–Martin periodinane (DMP) resulted in the formation of a complex mixture of products. Therefore, the Weinreb amide **22** was prepared and subsequently reduced with lithium aluminum hydride to furnish **4**.

Biological screening: With the 21 azanitriles (**1a–o**, **2** and **3a–e**) and aldehyde **4** in hand, we next evaluated the inhibitory activity of the library against cruzain and rhodesain in a fluorometric microplate assay with the substrate Z-Phe-Arg-AMC. For comparison, K11002, K11777, and Z-Phe-Ala-CHN_2 (**6a**) were also assayed under identical conditions.

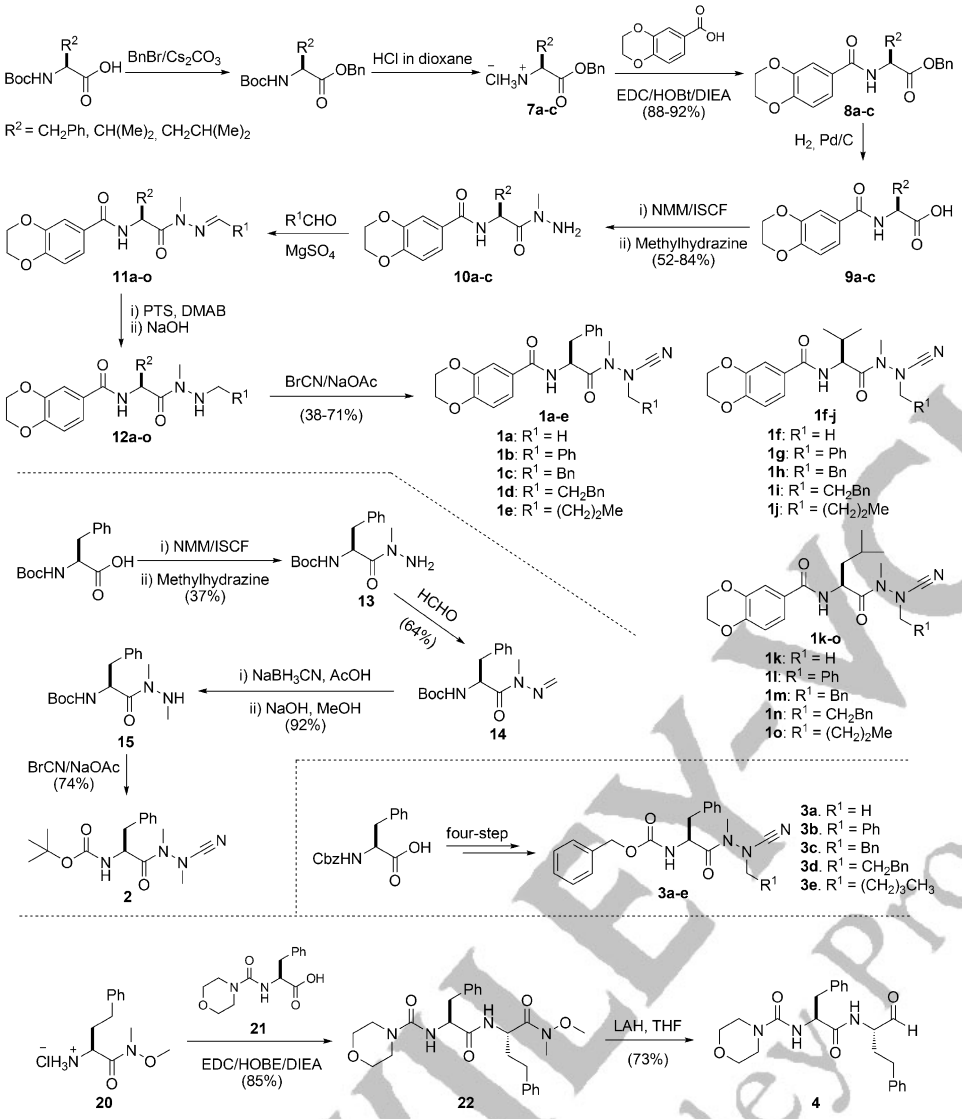

Scheme 1. Synthesis of inhibitors **1a–o**, **2**, **3a–e**, and **4** used in this study. THF = tetrahydrofuran, EDC = 1-ethyl-3-(3-dimethylaminopropyl)carbodiimide, HOBt = *N*-hydroxybenzotriazole, DIEA = *N*,*N*-diisopropylethylamine, NMM = *N*-methylmorpholine, ISCF = isobutyl chloroformate, PTS = *p*-toluenesulfonic acid, DMAB = dimethylamine borane, LAH = lithium aluminum hydride.

All compounds exhibited greater inhibitory capacity toward rhodesain than cruzain (Table 1 and Figure S2 A in the Supporting Information). The anti-cruzain and anti-rhodesain activities were well-correlated. This phenomenon is not surprising given the structural homology of these two enzymes. In general, compounds with Phe (**1a–e**) and Leu (**1k–o**) at the P_2 position were more active than compounds with Val (**1f–j**), whereas compounds with Leu (**1k–o**) exhibited higher potency against cruzain. For the P_1 position, compounds having a methyl group (**1a**, **1f**, and **1k**) yielded better results. Finally, changes made at the P_3 position conferred a subtle effect on enzyme selectivity, that is, **1a**, **2** versus **3a**, and **1b–d** versus **3b–d**. This indicates that, unlike previously assumed,[13] the P_3 position may be a recognition element for certain enzymes in the papain family. Indeed, a recent study in which a combination of optimized P_2 and P_3 substituents in azadipeptide nitriles was used, led to the identification of a picomolar cathepsin K inhibitor with remarkable selectivity over other cathepsins.[17] Compound **2**, bearing a Phe side chain and a Boc group at the P_2 and P_3 positions, respectively, was one of the most potent inhibitors against rhodesain (IC_{50} = 60 pM; $IC_{50\ cuzi}$ ■■do you mean cruzain? If not, please explain what "cuzi" refers to?■■ = 11.6 nM). Compound **1a** was also a highly potent inhibitor against rhodesain (IC_{50} = 140 pM, $IC_{50\ cuzi}$■■ = 8.5 nM). Another inhibitor with excellent inhibitory activity against rhodesain was **1k** (IC_{50} = 60 pM; $IC_{50\ cuzi}$■■ = 340 pM). As a control, IC_{50} values of K11002/K11777 were calculated for rhodesain (IC_{50} = 0.36 nM and 0.35 nM) and cruzain (IC_{50} = 6.6 nM and 4.1 nM). Interestingly, compound **4**, with an incorporated aldehyde "warhead", displayed a potency that was comparable to K11002/K11777 against both enzymes (IC_{50} values of 0.55 nM and 3.6 nM, respectively, against rhodesain and cruzain). Although we did not further evaluate the inhibitory activity of our compounds against TbCatB due to the unavailability of this enzyme, we were encouraged by the observation that some compounds show low picomolar IC_{50} values against rhodesain, and thereby decided to investigate their activities against live parasites (whole-organism-based screening). In this context, it is noteworthy that TbCatB was previously shown to be essential for *T. brucei* survival based on RNA interference studies in culture and in mice.[6,28] Whether rhodesain is essential for the parasite in culture is unclear, but the key role of rhodesain in *T. brucei* infection was clearly illustrated in experiments in which rhodesain-RNAi parasites were shown to be significantly less efficient in penetrating an in vitro model of the blood-brain barrier upon blockage by the cysteine protease inhibitor K11777.[9b] Consequently, these data validate rhodesain as a viable drug target in *T. brucei*.[29]

Table 1. In vitro inhibitory effects of the compounds tested against recombinant cruzain and rhodesain as well as *T. brucei*.[a]

Compound	IC_{50} [nM]		ED_{50} [μM]	
	Rhodesain	Cruzain	BSF	PCF
1a	0.14±0.06	8.5±0.002	nd	nd
1b	0.51±0.01	19.5±0.01	nd	nd
1c	1.86±0.01	101.6±0.005	nd	nd
1d	0.24±0.004	8.1±0.008	nd	nd
1e	1.34±0.02	52.2±0.02	nd	nd
1f	5.4±0.01	18.8±0.003	nd	nd
1g	15.8±0.001	133.6±0.02	nd	nd
1h	35.1±0.002	396.9±0.003	nd	nd
1i	54.0±0.01	410.6±0.001	nd	nd
1j	54.6±0.001	410.6±0.01	nd	nd
1k	0.06±0.001	0.34±0.004	nd	nd
1l	0.33±0.04	4.2±0.02	nd	nd
1m	0.71±0.001	9.8±0.004	nd	nd
1n	0.14±0.02	2.5±0.02	nd	nd
1o	0.33±0.02	8.4±0.002	nd	nd
2	0.06±0.008	11.6±0.02	nd	nd
3a	0.4±0.01	3.4±0.005	nd	nd
3b	0.19±0.02	8.4±0.01	1.1±0.3	0.4±0.2
3c	0.81±0.009	22.7±0.003	nd	nd
3d	2.0±0.002	115.7±0.002	1.2±0.3	0.7±0.1
3e	0.06±0.00	3.1±0.006	1.4±0.4	0.7±0.3
4	0.55±0.005	3.6±0.002	nd	nd
6a	3.1±0.4	9.3±0.2	nd	nd
K11002	0.36±0.02	6.6±0.001	5.6±0.4	7.3±0.3
K11777	0.35±0.03	4.1±0.005	0.9±0.3	5.8±0.4

[a] Data with standard errors were calculated from duplicate experiments by using seven different inhibitor concentrations. nd = Not determined.

We next evaluated the trypanocidal activities of these compounds in cell cultures of both the bloodstream form (BSF) and the procyclic form (PCF) of *T. brucei* by using a growth assay on a Guava PCA-96 system (Guava Technologies, USA) following the manufacturer's instructions. As shown in Figure 2, all compounds induced a potent, dose-dependent inhibition of parasite replication. As expected, most azanitriles were found to be significantly more potent than the three positive controls (K11002, K11777 and Z-Phe-Ala-CHN_2 (**6a**)). Overall, there were similarities in the structure–activity relationship (SAR) in this series of compounds between the recombinant enzymes (especially rhodesain) and *T. brucei*. Compounds **3a–e**, with Phe at the P_2 position and Cbz at the P_3 position, displayed the best parasite-killing activity against *T. brucei*. Similar to data obtained from rhodesain inhibition experiments, compounds having Phe (**1a–e**) and Leu (**1k–o**) at the P_2 position inhibited parasite growth better than compounds having Val (**1f–j**) at the same position. When compounds **1a–e** (with Phe at the P_2 position) and **1k–o** (with Leu at the P_2 position) were compared, no significant difference in anti-parasitic activity was observed. Notably, compound **2**, which has a Boc group at the P_3 position and exhibited an IC_{50} value of 60 pM against rhodesain, was comparatively less potent in its anti-parasitic activity than compounds **1a** and **3a** (which bear an aromatic amide and a Cbz group at the P_3 position, respectively). This suggests that the P_3 residue is important for the trypanocidal activity of these azanitriles. For all compounds tested, there was no clear difference in trypanocidal activity when the P_1 position was changed from a methyl group to other groups. This series of compounds, however, were able to block parasite growth much more effectively than K11002/K11777. These results did not entirely correlate with inhibition results obtained with recombinant rhodesain (Table 1), which might be due to differences in their cell permeability and/or the mechanism of action of these compounds. The exact reason is still under investigation. To quantitatively verify the above screening results against some of the compounds tested across a wider range of inhibitor concentrations, we subsequently obtained the ED_{50} values of selected compounds (**3b**, **3d**, **3e**, and K11777/K11002) against both life cycle stages of *T. brucei* (Table 1 and Figure S2B of the Supporting Information). Interestingly, our results clearly showed that these azanitriles (e.g., **3b**, **3d**, and **3e**) were approximately two-fold more active in blocking PCF parasite growth (ED_{50} values of 0.4, 0.7, and 0.7 μM, respectively, after 24 h) than BSF parasite growth (ED_{50} values of 1.1, 1.1, and 1.4 μM, respectively). Importantly, all of them displayed stronger trypanocidal activity than K11777 and K11002 in both PCF and BSF of *T. brucei*. In contrast, both K11777 and K11002 displayed slightly stronger trypanocidal activity in BSF (ED_{50} = 0.9 and 5.6 μM) than in PCF (ED_{50} = 5.8 and 7.3 μM). In this context, it is worth noting that the life cycle of *T. brucei* alternates between mammalian host stages and insect vector stages, which are coupled to extensive alterations in morphology and metabolism. Although the precise underlying mechanism for the above differences is presently unclear, they appear again to be related to differences in the cell permeability and/or cellular targets. Therefore, as described in the next paragraphs, we made an attempt to identify potential cellular targets (on and off) of some of the most potent compounds in *T. brucei*

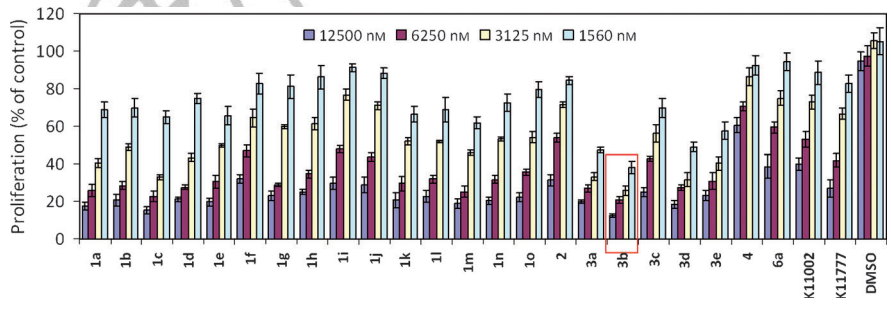

Figure 2. Dose-dependent, anti-trypanocidal effects of azanitriles (**1a–o**, **2**, and **3a–e**), aldehyde **4**, vinyl sulfones K11002 and K11777, as well as diazomethylketone Z-Phe-Ala-CHN_2 (**6a**) against the bloodstream form (BSF) of *T. brucei* using the Guava ViaCount assay after 24 h. PCF results against selected compounds are shown in the Supporting Information (Figure S2B). Results represent the average standard deviation from duplicate experiments.

by using activity-based protein profiling (ABPP) coupled to bioorthogonal click chemistry.[22,23] To this end, we have successfully made cell-permeable activity-based probes (ABPs) and used them for parasite-based proteome profiling and bioimaging experiments (see below). It should also be noted that, due to the high similarity between *T. cruzi* and *T. brucei*, these compounds/probes are possibly also effective against *T. cruzi*.

Design and synthesis of activity-based probes (ABPs): Our screening results thus far showed some of the azanitriles were highly potent inhibitors of cruzain/rhodesain, which was likely due to the covalent nature of these inhibitors in binding to the active site of the enzymes. These compounds possessed excellent trypanocidal activity in *T. brucei*, likely through inhibition of endogenous rhodesain/TbCatB activities, but they fell short in addressing the possibility that other cellular proteins present in the parasite proteome (for example, off-targets) might also be targeted. To facilitate a more detailed understanding of this novel class of inhibitors, we took advantage of the covalent nature of these compounds, and converted two hit compounds identified from our screening results, **3b**, and Z-Phe-Ala-CHN_2 (**6a**), into activity-based probes (ABPs) that would enable parasite-based proteome profiling and large-scale pull-down/LC-MS/MS analysis to identify potential cellular targets (on and off) based on our previously established protocols.[30] Compound **6a** was chosen as the positive control for our proteomic studies because this compound is a known covalent inhibitor that targets parasite cysteine proteases.[11] Its corresponding probe, **6b**, would thus make a suitable ABP for comparative profiling studies. Briefly, the two probes, **5** and **6b**, were designed and chemically synthesized (Scheme 2). In both cases, a terminal alkyne was introduced at a suitable position (for example, near the P_3 position) for subsequent click chemistry,[23] followed by in-gel fluorescence and bioimaging/pull-down experiments. We had previously found, from an independent study with natural-product-like probes,[30a,b] that only extremely conservative modifications ensured full retention of the native biological properties of the parent compounds (for example **3b** and **6a**). Probes **5** and **6b** were conveniently prepared from the key intermediate **23**, which was obtained in four steps from phenylalanine. The subsequent transformations leading to **5** were performed in a similar way to that of **3b**. Likewise, compound **23** was coupled with L-alanine methyl ester hydrochloride (**27**) to give the corresponding dipeptide, whereupon subsequent hydrolysis was carried out under basic conditions, giving **29b**. Its activation with isobutyl chloroformate in the presence of *N*-methylmorpholine and subsequent reaction of the mixed anhydride with diazomethane gave the diazomethylketone probe **6b**.

In situ proteome profiling: We first confirmed that compounds **5** and **6b** retained the full biological activities of their parent compounds (Figure 3A and Figure 3B); both the IC_{50} against recombinant rhodesain and dose-dependent inhibitory profiles against the growth of BSF/PCF of *T. brucei* were comparable to those of **3b** and **6a**, respectively. For example, probe **5** and compound **3b** displayed nearly identical IC_{50} values against rhodesain (0.21 and 0.19 nM, respectively; Figure 3A) and inhibitory profiles against *T. brucei* growth. Similar results were obtained for probe **6b** and compound **6a** (IC_{50} = 2.9 and 3.1 nM, respectively; for parasite inhibition profiles, compare Figure 3B and Figure 2). Taken together, these data showed that the introduction of a terminal alkyne handle in **3b** and **6a** did not noticeably affect their trypanocidal activities, and confirmed **5** and **6b** were suitable ABPs for subsequent target identification/profiling studies. We next compared the in situ proteome reactivity profiles of two probes by using live BSF and PCF following a previously optimized procedure.[10] Briefly, probes were directly added to the cell medium in which parasites were grown. After two hours, the parasites were washed (to remove excess probes), homogenized, incubated with rhodamine-azide under click chemistry conditions,[30] separated by sodium dodecyl sulfate-polyacrylamide gel electrophoresis (SDS-PAGE), and analyzed by in-gel

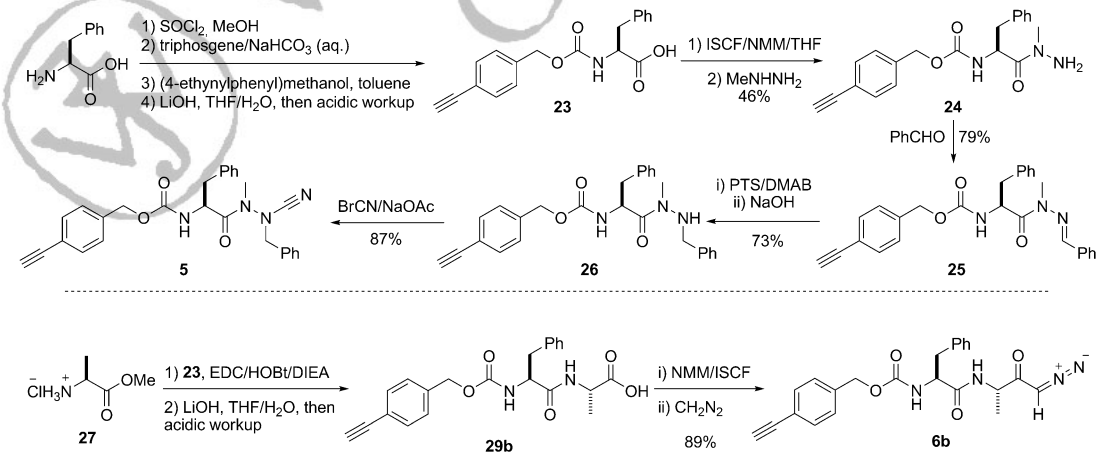

Scheme 2. Synthesis of activity-based probes (ABPs) **5** and **6b**.

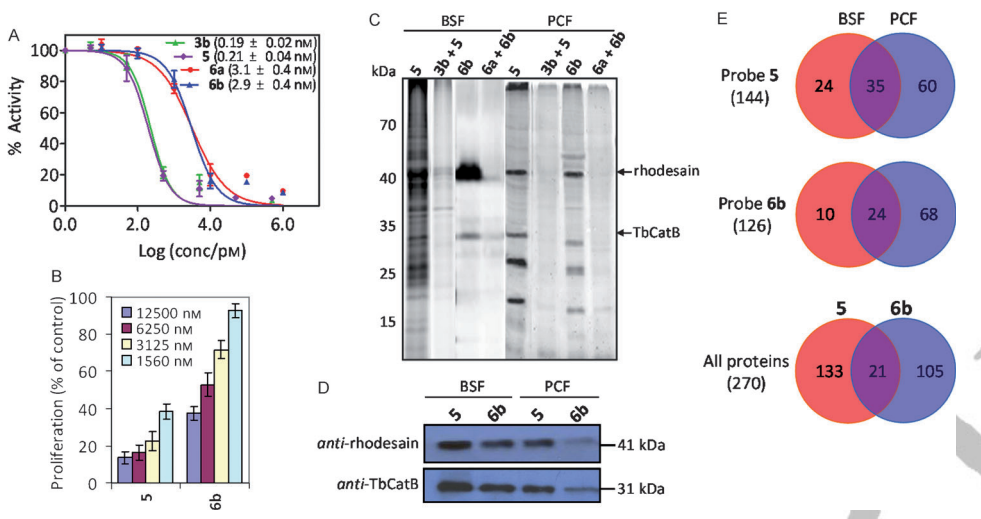

Figure 3. Biological evaluation of two ABPs (**5** and **6b**) in living *T. brucei*. A) IC_{50} curves of probes and their parent compounds against rhodesain. B) Dose-dependent, anti-trypanocidal effects of the probes against bloodstream forms of *T. brucei* after 24 h. Results represent the average standard deviation for duplicated independent trials. C) In situ proteome-profiling of probes (**5**, 1 μM; **6b**, 10 μM) against BSF and PCF of *T. brucei*. Compound **3b** (10 μM) or **6a** (100 μM) was added to selected lanes in competition experiments. Putative bands of labeled rhodesain and TbCatB are indicated with arrows. D) Western blotting validation of rhodesain and TbCatB labeled with **5** (1 μM) or **6b** (10 μM), following in situ labeling and affinity pull-down experiments. E) Venn diagram illustrating the numbers of proteins identified from *T. brucei* with probe **5** (1 μM) and **6b** (10 μM), after in situ labeling and large-scale pull-down/LC-MS/MS experiments.

fluorescence scanning (Figure 3C); both probes produced distinct fluorescently labeled bands, indicating that both class of compounds were, as expected, covalent inhibitors of their intended cellular targets. In general, comparable in situ proteome profiles were obtained for both probes in both forms of *T. brucei*, albeit with significant differences in relative reactivity (compare Figure 3 lanes 1 and 3 for BSF and lanes 5 and 7 for PCF). For example, 1 μM of **5** was able to give stronger fluorescence-labeling profiles than 10 μM of **6b**. These results correlated well with the relative potency of their trypanocidal activities. This observation, together with the fact that the fluorescence labeling of these two probes were efficiently inhibited by the addition of excess **3b** and **6a** (Figure 3, lanes 2, 4, 6, and 8), indicates that all the labeled proteins were likely true cellular targets of the probes, and that both probes had similar cellular targets in the parasites. On a related note, as seen in Figure 3 lanes 1/5 (for probe **5**) and lanes 3/7 (for probe **6b**), the in situ proteome reactivity profiles between BSF and PCF of the parasites, although similar, showed noticeable differences, suggesting the existence of both common and unique targets in the two forms of parasites.

The covalent labeling of the two expected cellular targets, rhodesain and TbCatB (ca. 41 and ca. 31 kDa; Figure 3C), were unequivocally verified by affinity pull-down/western blotting with the corresponding antibodies (Figure 3D). Also evident in Figure 3C and D is that the two probes labeled only the mature active enzyme form of rhodesain (ca. 41 kDa), and not its proform (ca. 48 kDa).[26a] In addition, the fluorescent TbCatB bands labeled by the two probes were detected more prominently in BSF than in PCF. This is consistent with previous findings that TbCatB was up-regulated in BSF.[6,31] Finally, to identify other proteins that were also covalently labeled by the two probes, we performed large-scale proteomic analyses using **5** and **6b** in both parasite forms by affinity pull-down followed by LC-MS/MS experiments (Table 2). All proteins were identified

Table 2. Representative proteins identified by probe **5** or **6b** in *T. brucei*.[a]

T. brucei gene	Protein name	Location	Detection	
			5	**6b**
Tb927.6.1000	cysteine peptidase precursor (CP), Clan CA, family C1, Cathepsin L-like**	L	both	both
Tb927.6.560	cysteine peptidase C (CPC), Clan CA, family C1, Cathepsin B-like**	L	BSF	BSF
Tb927.4.3950	cytoskeleton-associated protein CAP5.5, putative, cysteine peptidase, Clan CA, family C2, putative (CAP5.5)**	n/a	both	–
Tb11.47.0035	calpain-like cysteine peptidase, cysteine peptidase, Clan CA, family C2, putative**	n/a	BSF	–
Tb927.3.3410	aspartyl aminopeptidase	n/a	BSF	–
Tb927.5.1810	lysosomal/endosomal membrane protein p67 (p67)	L	BSF	–
Tb11.01.1350	S-adenosylhomocysteine hydrolase	n/a	PCF	–
Tb927.6.950	cysteinyl-tRNA synthetase	C	PCF	–
Tb927.8.2540	3-ketoacyl-CoA thiolase*	M	PCF	–
Tb927.8.1990	tryparedoxin peroxidase (TRYP2)	M	PCF	–
Tb10.6k15.2290	protein disulfide isomerase, bloodstream-specific protein 2 precursor (BS2)*	C	–	BSF
Tb10.70.5250	metacaspase MCA4, cysteine peptidase, Clan CD, family C13 (MCA4)**	N	–	BSF
Tb927.6.1260	proteasome beta-1 subunit (TbPSB1)*	n/a	–	BSF
Tb11.02.0100	carboxypeptidase	n/a	–	PCF
Tb11.01.3960	flagellar protein essential for flagellar pocket biogenesis (BILBO1)*	F	–	PCF
Tb927.3.2230	succinyl-CoA synthetase alpha subunit*	M	–	PCF
Tb11.02.4080	sterol 14-alpha-demethylase (CYP51)**	n/a	–	PCF

[a] L, C, N, M and F represent lysosome, cytoplasm, nucleus, mitochondrion and flagellum, respectively. n/a = Not available. Symbols in the protein name column: (*) sensitive to RNA interference; (**) putative drug target.

with a minimum protein score of 30 as well as at least four unique peptides; the results are summarized in Figure 3E. In total, 59 and 95 proteins were identified with probe **5** from BSF and PCF, respectively, of which 35 were detected in both parasitic forms. For probe **6b**, 34 and 92 proteins were identified in BSF and PCF, respectively, with 24 detected in both forms. When all proteins identified from both forms were pooled together, 133 and 105 were uniquely identified in BSF and PCF, respectively, and 21 were present in both forms. Among these proteins, some were nonspecific protein binders as a result of their "sticky" nature as well as their high endogenous expression level, such as carbohydrate-metabolism-related glycosomal proteins, although correct localization of glycosomal proteins has been shown to be essential for the survival of the bloodstream form as well as of the procyclic form of *T. brucei*. We therefore focused our attention on other candidate proteins having previously known nucleophilic cysteine residues in their active sites, because they are likely to be reactive towards both **5** and **6b**, and therefore may be true cellular targets of the corresponding parent compounds (**3b** and **6a**). As shown in Table 2, in addition to the expected proteins rhodesain and TbCatB, other proteins such as CAP5.5, calpain-like cysteine peptidase,[11] BS2, MCA4, and one proteosome subunit were identified only in BSF with either **5** or **6b**.[32] Of note, sterol 14-alpha-demethylase (CYP51),[33] which has recently been validated as a potential target for anti-trypanosomal therapy, was identified only with **6b** in both forms. Additionally, we have identified several proteins, including 3-ketoacyl-CoA thiolase,[34] BILBO1,[35] and succinyl-CoA synthetase alpha,[36] all of which were previously reported to be essential for parasite survival from RNAi experiments. Finally, it should be noted that the LC-MS/MS-based results obtained above should only be used as preliminary data; owing to the highly complex cellular environment and the intrinsic limitations of affinity pull-down/mass spectrometric experiments, false positives and nonspecific protein binding could be minimized but not eliminated. Consequently, proper follow-up studies and validation experiments will be needed before any biological conclusions can be made for some of these protein hits.

Cellular imaging using activity-based probes: Having accomplished putative target identification using the corresponding ABPs **5** and **6b**, we next investigated whether these probes could be used for drug uptake studies, as well as visualization of their sub-cellular distribution and potential cellular targets in live parasites (both BSF and PCF). To do this, live parasites were treated with probe **5** or **6b**, fixed, and reacted in situ with rhodamine-azide (Figure 4). Consistent with in situ labeling profiles, as low as 0.1 μM of probe **5** was sufficient to stain the parasites strongly, rendering them visible under a confocal fluorescence microscope (Figure 4A, Panels b and f), whereas 10 μM of **6b** was required to produce fluorescent images with comparable probe labelling intensity (Figure 4A, Panels d and h). There was no other noticeable difference in the cellular uptake of the two

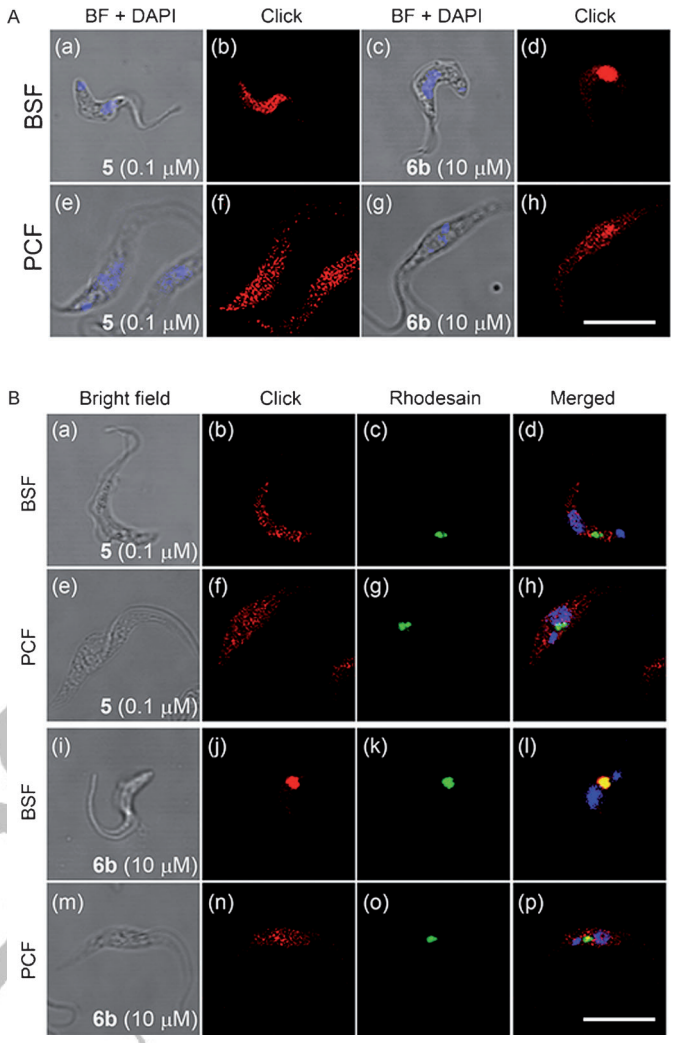

Figure 4. Fluorescence microscopy of A) cellular uptake and B) sub-cellular localization of the probes in BSF and PCF of *T. brucei*. Live parasites were treated with **5** (0.1 μM) or **6b** (10 μM) for 2 h, reacted with rhodamine-azide (10 μM) in situ under click chemistry conditions, and then imaged. A) Panels a, c, e and g: merged images of bright-field with stained nuclei (DAPI; in blue); Panels b, d, f and h: 554 nm channel (pseudocolored in red) detecting cellular uptake of the probe. B) Panels a, e, i and m: bright-field images; Panels b, f, j and n: 554 nm channel (pseudocolored in red) detecting cellular localization of the probe; Panels c, g, k and o: Immunofluorescence (IF) staining at 488 nm channel (pseudocolored in green) to detect cellular localization of rhodesain. Anti-rhodesain primary antibody and FITC-conjugated anti-rabbit IgG secondary antibody were used; Panels d, h, l and p: merged images of Panels b/c, f/g, j/k, and n/o together with stained nuclei (DAPI; in blue). All images were acquired under the same settings. Scale bar = 10 μm.

probes between BSF and PCF parasites. The sub-cellular distribution of the two probes, however, were notably different (Figure 4B); probe **6b** stained mostly lysosomal compartments of the BSF parasites, which was expected for a probe designed to target the endocytic cysteine proteases, rhodesain/TbCatB (Figure 4, Panel j). This result was further confirmed by immunofluorescence (IF) experiments with the anti-rhodesain antibody (Figure 4, Panel k).[10] Interestingly, the same probe showed mostly cytosolic distribution

in PCF parasites (Figure 4, Panel n). Probe **5**, on the other hand, did not appear to entirely colocalize with rhodesain (Figure 4, Panels d and h), and showed both lysosomal and cytosolic distribution in both BSF and PCF parasites (Figure 4, Panels b and f). Surprisingly, staining of HepG2 cells (Human hepatocellular liver carcinoma) with the probes revealed that **5** (at 1 μM) resided mostly in lysosomal compartments and colocalized with cathepsin L (see Figure S6 in the Supporting Information). On the other hand, even as high as 50 μM of **6b** only weakly stained HepG2 cells under similar conditions. In this context, it is noteworthy that cathepsin L is a lysosomal protease that is involved in all stages of cancer progression, including growth, antigiogenesis, invasion, and metastasis.[37] Recent research on cathepsin L also shows that proteolysis by this enzyme is required for entry and replication of the SARS and Ebola viruses in human cells.[38] Collectively, these results demonstrate that our newly synthesized ABPs could be used as potential cell-permeable bioimaging agents to study drug uptake and sub-cellular distribution.

Conclusion

We have synthesized a focused library of azanitrile-containing compounds and screened them for inhibitory activities against recombinant cruzain and rhodesain, as well as for their trypanocidal activities in both BSF and PCF of *T. brucei*. All compounds exhibited excellent activities and showed promise as potential anti-parasitic agents. By comparing the structure–activity relationship (SAR) of these compounds, inhibition of rhodesain protease activity and trypanocidal activities were found to be well-correlated. The rational approach taken to design this novel class of compounds may provide a starting point for future development of compounds that are suitable for therapeutic applications, and be used to address selectivity profiles of different classes of cysteine protease inhibitors (i.e., azanitriles vs. diazomethylketones).[39] Furthermore, based on the most potent hits from our screening results, two activity-based probes, **5** and **6b**, were subsequently developed. These cell-permeable probes enabled parasite-based proteome profiling/identification of potential cellular targets (on and off) of the parent compounds, and unequivocally confirmed that both rhodesain and TbCatB were targets of our compounds. The probes could be used in cell imaging experiments for further assessment of drug uptake and sub-cellular distribution. Clearly, additional studies will be required for further target validation, as well as to determine drug efficacy and toxicity in animal models. Furthermore, we expect the azadipeptide nitrile inhibitors reported in this study will likely be potent against human cathepsins (see Figure S3 in the Supporting Information and references [16] and [19]) due to the high sequence homology of these enzymes with rhodesain/cruzain. This, however, should not deter further investigations into their use as potential anti-parasitic agents. Previous studies clearly indicated that preferential inhibition of parasite cysteine proteases over human cathepsins is possible in infected human cells due to parasite localization, for example, parasites reside in the cytoplasm of host cells, whereas the cathepsins are located in the less accessible lysosomes.[12c] In fact, K11777—currently the most advanced inhibitor in pre-clinical trials against Chagas disease—also potently inhibits a variety of recombinant human cathepsins.[10,12a] Nevertheless, Gutschow et al. have recently shown that it is possible to achieve selective cathepsin inhibition by fine-tuning the structure of azadipeptide nitriles.[17b]

Experimental Section

Chemistry: Unless otherwise stated, all reactions were carried out under an atmosphere of dry argon or nitrogen in dried glassware. Indicated reaction temperatures refer to those of the reaction bath; room temperature (RT) is noted as 25 °C. Commercially available starting materials and regents were purchased from Aldrich, Alfa Aesar, or Fluka and used as received. Tetrahydrofuran (THF) was distilled over sodium benzophenone and used immediately. Reaction progress was monitored by analytical thin layer chromatography (TLC) on pre-coated silica plates (Merck 60 F254, 250 μm thickness) and spots were visualized by irradiation under a 254 nm UV lamp, and by treatment with ceric ammonium molybdate, basic $KMnO_4$, or iodine. ^1H and ^{13}C NMR spectra were recorded with a Bruker Avance 300 MHz, DPX-300 MHz, or DPX-500 MHz NMR spectrometer. Chemical shifts are reported in ppm relative to internal standard tetramethylsilane (TMS) or residual solvent peaks ($CDCl_3$ δ = 7.26, 77.00 ppm; $[D_6]$DMSO δ = 2.50, 39.50 ppm for ^1H and ^{13}C, respectively). Data are reported as follows: chemical shift, multiplicity (s = singlet, d = doublet, t = triplet, q = quartet, br = broad, m = multiplet), coupling constants, and number of protons. Mass spectra were obtained with a Shimadzu IT-TOF-MS system. The syntheses and characterizations of **16**, **17b, 17c**, **18e**, **18a–c**, **18e**, **3a–c**, **3e**, **19**, **21**, and **23** were previously reported.[10,16]

(*S*)-*N*-[1-(2-Cyano-1,2-dimethylhydrazinyl)-1-oxo-3-phenylpropan-2-yl]-2,3-dihydrobenzo[b][1,4]dioxine-6-carboxamide (1a): This general procedure was adapted from a prior publication.[16] Anhydrous sodium acetate (164 mg, 2.0 mmol) and cyanogen bromide (106 mg, 1.0 mmol) were added to a stirred solution of **12a** (185 mg, 0.5 mmol) in anhydrous MeOH (10 mL). The mixture was stirred at RT for 12 h, then two additional equivalents of cyanogen bromide (106 mg, 1.0 mmol) were added and stirring was continued for 24 h. The solvent was removed under reduced pressure, the oily residue was suspended in H_2O (10 mL), and the solution was adjusted to pH 1–2 (10% $KHSO_4$), extracted with EtOAc (5 × 20 mL), and the combined organic layers were washed with H_2O, sat. $NaHCO_3$, and brine. The solvent was dried (Na_2SO_4) and evaporated. Purification by flash column chromatography (silica gel) using 20 to 50% EtOAc in hexanes gave **1a** as a white solid (146 mg, 74%). ^1H NMR (500 MHz, $CDCl_3$): δ = 3.00–3.23 (m, 2H), 3.24 (s, 3H), 3.33 (s, 3H), 4.26 (dd, J = 5.0, 15.0 Hz, 4H), 5.41–5.46 (m, 1H), 6.71 (d, J = 5.0 Hz, 1H), 6.84 (d, J = 10.0 Hz, 1H), 7.18–7.34 ppm (m, 7H); ^{13}C NMR (126 MHz, $CDCl_3$): δ = 29.7, 30.5, 37.9, 41.1, 50.7, 64.1, 64.5, 113.5, 116.6, 117.2, 120.6, 126.7, 127.3, 128.8, 129.2, 129.6, 135.6, 143.3, 146.8, 166.7, 173.4 ppm; LC-IT-TOF/MS: m/z calcd for $C_{21}H_{22}N_4O_4$: 395.1641 $[M+H]^+$; found: 395.1654.

(*S*)-*N*-[1-(2-Benzyl-2-cyano-1-methylhydrazinyl)-1-oxo-3-phenylpropan-2-yl]-2,3-dihydrobenzo[b][1,4]dioxine-6-carboxamide (1b): Prepared according to the general procedure using **12b** (102 mg, 0.23 mmol), sodium acetate (75 mg, 0.9 mmol), and cyanogen bromide (96 mg, 0.9 mmol) in anhydrous methanol (10 mL) to afford **1b** (84 mg, 79%) as a white solid. ^1H NMR (500 MHz, $CDCl_3$): δ = 2.97–3.14 (m, 2H), 3.16 (s, 3H), 4.23–4.27 (m, 4H), 4.64 (s, 2H), 5.52–5.56 (m, 1H), 6.84–6.87 (m, 2H), 7.17–7.53 ppm (m, 13H); ^{13}C NMR (126 MHz, $CDCl_3$): δ = 32.3, 37.8, 51.3, 58.9, 64.1, 64.5, 112.3, 115.9, 116.6, 117.2, 120.6, 126.8, 127.2, 127.4, 128.2, 128.7, 128.8, 129.1, 129.3, 129.4, 129.5, 129.7, 130.3, 131.5, 135.8, 143.3,

146.7, 166.8, 173.8 ppm; LC-IT-TOF/MS: *m/z* calcd for $C_{27}H_{26}N_4O_4$: 471.1954 $[M+H]^+$; found: 471.1968.

(*S*)-*N*-[1-(2-Cyano-1-methyl-2-phenethylhydrazinyl)-1-oxo-3-phenylpropan-2-yl]-2,3-dihydrobenzo[b][1,4]dioxine-6-carboxamide (1c): Prepared according to the general procedure using **12c** (138 mg, 0.3 mmol), sodium acetate (100 mg, 1.2 mmol), and cyanogen bromide (128 mg, 1.2 mmol) in anhydrous methanol (10 mL) to afford **1c** (118 mg, 81%) as a white solid. ^{1}H NMR (500 MHz, $CDCl_3$): δ = 2.85–2.89 (m, 2H), 3.06–3.16 (m, 2H), 3.18 (s, 3H), 3.71–3.76 (m, 1H), 3.83–3.89 (m, 1H), 4.26 (dd, J = 5.0, 10.0 Hz, 4H), 5.11–5.16 (m, 1H), 6.38 (d, J = 10.0 Hz, 1H), 6.85 (d, J = 10.0 Hz, 1H), 7.03 (d, J = 10.0 Hz, 1H), 7.15–7.36 ppm (m, 11H); ^{13}C NMR (126 MHz, $CDCl_3$): δ = 31.6, 32.9, 37.7, 50.6, 54.8, 64.2, 64.5, 112.3, 116.6, 117.3, 120.5, 126.9, 127.2, 127.3, 128.8, 128.9, 129.0, 129.2, 129.5, 135.4, 136.2, 143.4, 146.8, 166.6, 173.4 ppm; LC-IT-TOF/MS: *m/z* calcd for $C_{28}H_{28}N_4O_4$: 485.2111 $[M+H]^+$; found: 485.2102.

(*S*)-*N*-{1-[2-Cyano-1-methyl-2-(3-phenylpropyl)hydrazinyl]-1-oxo-3-phenylpropan-2-yl}-2,3-dihydrobenzo[b][1,4]dioxine-6-carboxamide (1d): Prepared according to the general procedure using **12d** (160 mg, 0.34 mmol), sodium acetate (112 mg, 1.4 mmol), and cyanogen bromide (143 mg, 1.4 mmol) in anhydrous methanol (10 mL) to afford **1d** (123 mg, 73%) as a white solid. ^{1}H NMR (500 MHz, $CDCl_3$): δ = 2.10–2.16 (m, 2H), 2.74–2.86 (m, 2H), 3.00–3.04 (m, 2H), 3.22 (s, 3H), 3.45–3.55 (m, 2H), 4.26 (dd, J = 5.0, 10.0 Hz, 4H), 5.44–5.48 (m, 1H), 6.63 (d, J = 10.0 Hz, 1H), 6.84 (d, J = 10.0 Hz, 1H), 7.13–7.33 ppm (m, 11H); ^{13}C NMR (126 MHz, $CDCl_3$): δ = 28.2, 31.6, 32.6, 38.0, 50.8, 53.6, 64.2, 64.6, 112.5, 116.6, 117.3, 120.6, 126.4, 126.9, 127.4, 128.4, 128.7, 128.8, 129.2, 129.6, 135.7, 140.0, 143.4, 146.8, 166.6, 168.4, 173.5 ppm; LC-IT-TOF/MS: *m/z* calcd for $C_{29}H_{30}N_4O_4$: 499.2267 $[M+H]^+$; found: 499.2329.

(*S*)-*N*-[1-(2-Butyl-2-cyano-1-methylhydrazinyl)-1-oxo-3-phenylpropan-2-yl]-2,3-dihydrobenzo[b][1,4]dioxine-6-carboxamide (1e): Prepared according to the general procedure using **12e** (155 mg, 0.38 mmol), sodium acetate (123 mg, 1.5 mmol), and cyanogen bromide (160 mg, 1.5 mmol) in anhydrous methanol (10 mL) to afford **1e** (113 mg, 69%) as a white solid. ^{1}H NMR (500 MHz, $CDCl_3$): δ = 0.99 (t, J = 10.0 Hz, 3H), 1.47–1.56 (m, 2H), 1.74–1.83 (m, 2H), 2.96–3.21 (m, 2H), 3.26(s, 3H), 3.42- 3.54 (m, 2H), 4.25 (d, J = 10.0 Hz, 4H), 5.39–5.43 (m, 1H), 6.79–6.87 (m, 2H), 7.18–7.33 ppm (m, 6H); ^{13}C NMR (126 MHz, $CDCl_3$): δ = 13.7, 19.6, 19.8, 28.6, 31.5, 37.7, 50.9, 53.8, 64.1, 64.5, 112.5, 116.6, 117.2, 120.6, 126.9, 127.2, 128.7, 129.2, 129.5, 135.8, 143.3, 146.7, 166.6, 173.5 ppm; LC-IT-TOF/MS: *m/z* calcd for $C_{24}H_{28}N_4O_4$: 437.2111 $[M+H]^+$; found: 437.2102.

(*S*)-*N*-[1-(2-Cyano-1,2-dimethylhydrazinyl)-3-methyl-1-oxobutan-2-yl]-2,3-dihydrobenzo[b][1,4]dioxine-6-carboxamide (1f): Prepared according to the general procedure using **12f** (106 mg, 0.33 mmol), sodium acetate (107 mg, 1.3 mmol), and cyanogen bromide (138 mg, 1.3 mmol) in anhydrous methanol (10 mL) to afford **1f** (80 mg, 70%) as a white solid. ^{1}H NMR (500 MHz, $CDCl_3$): δ = 1.04 (d, J = 10.0 Hz, 3H), 1.07 (d, J = 10.0 Hz, 3H), 2.09–2.17 (m, 1H), 3.24 (s, 3H), 3.32 (s, 3H), 4.26–4.30 (m, 4H), 5.10–5.13 (m, 1H), 6.57 (d, J = 10.0 Hz, 1H), 6.88 (d, J = 5.0 Hz, 1H), 7.29–7.35 ppm (m, 2H); ^{13}C NMR (126 MHz, $CDCl_3$): δ = 18.1, 19.6, 30.2, 31.4, 41.2, 54.0, 64.2, 64.5, 113.9, 116.6, 117.3, 120.6, 127.0, 143.4, 146.8, 166.9, 173.0 ppm; LC-IT-TOF/MS: *m/z* calcd for $C_{17}H_{22}N_4O_4$: 347.1641 $[M+H]^+$; found: 347.347.1648.

(*S*)-*N*-[1-(2-Benzyl-2-cyano-1-methylhydrazinyl)-3-methyl-1-oxobutan-2-yl]-2,3-dihydrobenzo[b][1,4]dioxine-6-carboxamide (1g): Prepared according to the general procedure using **12g** (140 mg, 0.35 mmol), sodium acetate (115 mg, 1.4 mmol), and cyanogen bromide (149 mg, 1.4 mmol) in anhydrous methanol (10 mL) to afford **1g** (115 mg, 78%) as a white solid. ^{1}H NMR (500 MHz, $CDCl_3$): δ = 1.03 (d, J = 10.0 Hz, 3H), 1.05 (d, J = 10.0 Hz, 3H), 2.10–2.17 (m, 1H), 3.13 (s, 3H), 4.29 (dd, J = 5.0, 10.0 Hz, 4H), 4.62 (dd, J = 15.0, 20.0 Hz, 2H), 5.26–5.30 (m, 1H), 6.54 (d, J = 10.0 Hz, 1H), 6.91 (d, J = 5.0 Hz, 1H), 7.30–7.44 (m, 6H), 7.55 ppm (d, J = 10.0 Hz, 1H); ^{13}C NMR (126 MHz, $CDCl_3$): δ = 18.0, 19.7, 31.5, 32.2, 54.2, 59.0, 64.2, 64.6, 112.7, 116.7, 117.3, 120.6, 127.2, 129.3, 129.7, 130.3, 131.6, 143.4, 146.8, 167.0, 174.1 ppm; LC-IT-TOF/MS: *m/z* calcd for $C_{23}H_{26}N_4O_4$: 423.1594 $[M+H]^+$; found: 423.1606.

(*S*)-*N*-[1-(2-Cyano-1-methyl-2-phenethylhydrazinyl)-3-methyl-1-oxobutan-2-yl]-2,3-dihydrobenzo[b][1,4]dioxine-6-carboxamide (1h): Prepared according to the general procedure using 12h (136 mg, 0.33 mmol), sodium acetate (108 mg, 1.3 mmol), and cyanogen bromide (141 mg, 1.3 mmol) in anhydrous methanol (10 mL) to afford **1h** (97 mg, 67%) as a white solid. ^{1}H NMR (500 MHz, $CDCl_3$): δ = 0.89 (t, J = 10.0 Hz, 6H), 1.94–2.04 (m, 1H), 3.06–3.13 (m, 2H), 3.19 (s, 3H), 3.60–3.73 (m, 1H), 3.84–3.89 (m, 1H), 4.27–4.30 (m, 4H), 4.72 (t, J = 10.0, 1H), 6.36 (d, J = 10.0 Hz, 1H), 6.89 (d, J = 10 Hz, 1H), 7.23–7.38 ppm (m, 7H); ^{13}C NMR (126 MHz, $CDCl_3$): δ = 17.9, 19.5, 31.0, 31.4, 32.9, 54.1, 54.8, 64.2, 64.6, 112.6, 116.6, 117.3, 120.5, 127.1, 127.2, 128.8, 129.2, 136.3, 143.4, 146.7, 166.9, 174.0 ppm; LC-IT-TOF/MS: *m/z* calcd for $C_{24}H_{28}N_4O_4$: 437.2111 $[M+H]^+$; found: 437.2121.

(*S*)-*N*-{1-[2-Cyano-1-methyl-2-(3-phenylpropyl)hydrazinyl]-3-methyl-1-oxobutan-2-yl}-2,3-dihydrobenzo[b][1,4]dioxine-6-carboxamide (1i): Prepared according to the general procedure using **12i** (127 mg, 0.3 mmol), sodium acetate (98 mg, 1.2 mmol), and cyanogen bromide (127 mg, 1.2 mmol) in anhydrous methanol (10 mL) to afford **1i** (101 mg, 75%) as a white solid. ^{1}H NMR (500 MHz, $CDCl_3$): δ = 1.02 (d, J = 5.0 Hz, 3H), 1.08 (d, J = 5.0 Hz, 3H), 2.09–2.18 (m, 3H), 2.78–2.85 (m, 2H), 3.21 (s, 3H), 3.43–3.51 (m, 2H), 4.26 (dd, J = 5.0, 10.0 Hz, 4H), 5.18 (dd, J = 5.0, 10.0 Hz, 1H), 6.54 (d, J = 10.0 Hz, 1H), 6.89 (d, J = 10 Hz, 1H), 7.19–7.34 ppm (m, 7H); ^{13}C NMR (126 MHz, $CDCl_3$): δ = 17.8, 19.7, 28.1, 31.38, 31.42, 32.6, 53.6, 53.9, 64.2, 64.5, 113.7, 116.6, 117.3, 120.5, 126.3, 127.2, 128.3, 128.6, 140.1, 143.4, 146.7, 166.8, 174.0 ppm; LC-IT-TOF/MS: *m/z* calcd for $C_{25}H_{30}N_4O_4$: 451.2267 $[M+H]^+$; found: 451.2284.

(*S*)-*N*-[1-(2-Butyl-2-cyano-1-methylhydrazinyl)-3-methyl-1-oxobutan-2-yl]-2,3-dihydrobenzo[b][1,4]dioxine-6-carboxamide (1j): Prepared according to the general procedure using **12j** (124 mg, 0.34 mmol), sodium acetate (112 mg, 1.4 mmol), and cyanogen bromide (144 mg, 1.4 mmol) in anhydrous methanol (10 mL) to afford **1j** (94 mg, 71%) as a white solid. ^{1}H NMR (500 MHz, $CDCl_3$): δ = 1.02 (d, J = 5.0 Hz, 3H), 1.08 (d, J = 5.0 Hz, 3H), 1.49–1.58 (m, 2H), 1.73–1.81 (m, 2H), 2.13–2.19 (m, 1H), 3.24 (s, 3H), 3.37–3.50 (m, 2H), 4.26–4.30 (m, 4H), 5.14 (dd, J = 5.0, 10.0 Hz, 1H), 6.54 (d, J = 5.0 Hz, 1H), 6.89 (d, J = 10.0 Hz, 1H), 7.28–7.34 ppm (m, 2H); ^{13}C NMR (126 MHz, $CDCl_3$): δ = 13.7, 17.6, 19.7, 19.8, 53.8, 54.0, 64.2, 64.5, 112.7, 116.6, 117.3, 120.5, 127.2, 143.4, 146.7, 166.8, 173.9 ppm; LC-IT-TOF/MS: *m/z* calcd for $C_{20}H_{28}N_4O_4$: 389.2111 $[M+H]^+$; found: 389.2134.

(*S*)-*N*-[1-(2-Cyano-1,2-dimethylhydrazinyl)-4-methyl-1-oxopentan-2-yl]-2,3-dihydrobenzo[b][1,4]dioxine-6-carboxamide (1k): Prepared according to the general procedure using **12k** (118 mg, 0.35 mmol), sodium acetate (115 mg, 1.4 mmol), and cyanogen bromide (149 mg, 1.4 mmol) in anhydrous methanol (10 mL) to afford **1k** (97 mg, 77%) as a white solid. ^{1}H NMR (500 MHz, $CDCl_3$): δ = 1.00 (d, J = 5.0 Hz, 3H), 1.05 (d, J = 5.0 Hz, 3H), 1.56–1.81 (m, 3H), 3.23 (s, 3H), 3.34 (s, 3H), 4.26–4.30 (m, 4H), 5.23–5.28 (m, 1H), 6.58 (d, J = 10.0 Hz, 1H), 6.88 (d, J = 10.0 Hz, 1H), 7.27–7.32 ppm (m, 2H); ^{13}C NMR (126 MHz, $CDCl_3$): δ = 21.5, 32.3, 25.1, 29.7, 30.5, 41.0, 41.3, 48.2, 64.2, 64.5, 113.6, 116.6, 117.3, 120.6, 126.8, 143.4, 146.8, 167.0, 174.7 ppm; LC-IT-TOF/MS: *m/z* calcd for $C_{18}H_{24}N_4O_4$: 361.1798 $[M+H]^+$; found: 361.1808.

(*S*)-*N*-[1-(2-Benzyl-2-cyano-1-methylhydrazinyl)-4-methyl-1-oxopentan-2-yl]-2,3-dihydrobenzo[b][1,4]dioxine-6-carboxamide (1l): Prepared according to the general procedure using **12l** (132 mg, 0.32 mmol), sodium acetate (106 mg, 1.3 mmol), and cyanogen bromide (138 mg, 1.3 mmol) in anhydrous methanol (10 mL) to afford **1l** (131 mg, 81%) as a white solid. ^{1}H NMR (500 MHz, $CDCl_3$): δ = 0.96 (t, J = 5.0 Hz, 6H), 1.50–1.81 (m, 3H), 3.14 (s, 3H), 4.28 (dd, J = 5.0, 15.0 Hz, 4H), 4.63 (s, 2H), 5.41–5.45 (m, 1H), 6.67 (d, J = 10.0 Hz, 1H), 6.89 (d, J = 10.0 Hz, 1H), 7.31–7.57 ppm (m, 7H); ^{13}C NMR (126 MHz, $CDCl_3$): δ = 21.4, 23.3, 25.0, 32.3, 41.3, 48.4, 58.9, 64.2, 64.6, 112.4, 116.7, 117.3, 120.7, 127.0, 127.4, 128.8, 129.3, 129.8, 130.4, 131.5, 143.4, 146.8, 167.1, 175.1 ppm; LC-IT-TOF/MS: *m/z* calcd for $C_{24}H_{28}N_4O_4$: 437.2111 $[M+H]^+$; found: 437.2124.

(*S*)-*N*-[1-(2-Cyano-1-methyl-2-phenethylhydrazinyl)-4-methyl-1-oxopentan-2-yl]-2,3-dihydrobenzo[b][1,4]dioxine-6-carboxamide (1m): Prepared according to the general procedure using **12m** (132 mg, 0.31 mg), sodium acetate (98 mg, 1.2 mmol), and cyanogen bromide (127 mg, 1.2 mmol) in anhydrous methanol (10 mL) to afford **1m** (110 mg, 79%) as a white solid. ^{1}H NMR (500 MHz, $CDCl_3$): δ = 0.91 (d, J = 5.0 Hz, 3H), 0.93 (d, J = 5.0 Hz, 3H), 1.48–1.69 (m, 3H), 3.11–3.14 (m, 2H), 3.16 (s, 3H), 3.69–3.74 (m, 1H), 3.81–3.87 (m, 1H), 4.25–4.29 (m, 4H), 5.11–5.15 (m, 1H),

6.58 (d, $J=5.0$ Hz, 1H), 6.87 (d, $J=10.0$ Hz, 1H), 7.23–7.35 ppm (m, 7H); ^{13}C NMR (126 MHz, $CDCl_3$): $\delta=21.5$, 23.2, 25.1, 31.6, 33.0, 41.1, 48.3, 54.9, 64.2, 64.5, 112.4, 116.6, 117.2, 120.6, 127.0, 127.2, 128.8, 129.0, 136.1, 143.3, 146.7, 167.0, 175.0 ppm; LC-IT-TOF/MS: m/z calcd for $C_{25}H_{30}N_4O_4$: 451.2267 $[M+H]^+$; found: 451.2260.

(*S*)-*N*-{1-[2-Cyano-1-methyl-2-(3-phenylpropyl)hydrazinyl]-4-methyl-1-oxopentan-2-yl}-2,3-dihydrobenzo[b][1,4]dioxine-6-carboxamide (1n): The general procedure was followed using **12n** (123 mg, 0.28 mmol), sodium acetate (92 mg, 1.1 mmol), and cyanogen bromide (117, 1.1 mmol) in anhydrous methanol (10 mL) to afford **1n** (95 mg, 73%) as a white solid. ^{1}H NMR (500 MHz, $CDCl_3$): $\delta=0.98$ (d, $J=5.0$ Hz, 3H), 1.03 (d, $J=5.0$ Hz, 3H), 1.57–1.67 (m, 2H), 1.80–1.81 (m, 1H), 2.11–2.17 (m, 2H), 2.77–2.86 (m, 2H), 3.21 (s, 3H), 3.47–3.56 (m, 2H), 4.25–4.29 (m, 4H), 5.28–5.33 (m, 1H), 6.68 (d, $J=10.0$ Hz, 1H), 6.88 (d, $J=5.0$ Hz, 1H), 7.21–7.32 ppm (m, 7H); ^{13}C NMR (126 MHz, $CDCl_3$): $\delta=21.5$, 23.3, 25.1, 28.2, 31.5, 32.6, 41.2, 48.3, 53.4, 61.1, 64.5, 112.5, 116.6, 117.2, 120.6, 126.4, 127.0, 128.3, 128.6, 140.1, 143.3, 146.7, 166.9, 175.0 ppm; LC-IT-TOF/MS: m/z calcd for $C_{26}H_{32}N_4O_4$: 465.2424 $[M+H]^+$; found: 465.2638.

(*S*)-*N*-[1-(2-Butyl-2-cyano-1-methylhydrazinyl)-4-methyl-1-oxopentan-2-yl]-2,3-dihydrobenzo[b][1,4]dioxine-6-carboxamide (1o): Prepared according to the general procedure using **12o** (132 mg, 0.35 mmol), sodium acetate (115 mg, 1.4 mmol), and cyanogen bromide (148 mg, 1.4 mmol) in anhydrous methanol (10 mL) to afford **1o** (94 mg, 67%) as a white solid. ^{1}H NMR (500 MHz, $CDCl_3$): $\delta=0.98$–1.05 (m, 9H), 1.50–1.82 (m, 7H), 3.23 (s, 3H), 3.41–3.53 (m, 2H), 4.26–4.30 (m, 4H), 5.24–5.29 (m, 1H), 6.58 (d, $J=10.0$ Hz, 1H), 6.88 (d, $J=5.0$ Hz, 1H), 7.28–7.32 ppm (m, 2H); ^{13}C NMR (126 MHz, $CDCl_3$): $\delta=13.7$, 19.8, 21.4, 23.3, 25.1, 28.7, 31.5, 41.3, 48.3, 53.7, 64.2, 64.5, 112.6, 116.6, 117.2, 120.6, 127.0, 143.4, 146.7, 166.9, 174.9 ppm; LC-IT-TOF/MS: m/z calcd for $C_{21}H_{30}N_4O_4$: 403.2267 $[M+H]^+$; found: 403.2314.

(*S*)-*tert*-Butyl [1-(2-Cyano-1,2-dimethylhydrazinyl)-1-oxo-3-phenylpropan-2-yl]carbamate (2): Prepared according to the general procedure using **15** (307 mg, 1.0 mmol), anhydrous sodium acetate (230 mg, 3 mmol), and cyanogen bromide (350 mg, 3.3 mmol) in anhydrous MeOH (25 mL) to afford **2** (246 mg, 74%) as a pale-yellow solid. ^{1}H NMR (500 MHz, $CDCl_3$): $\delta=1.37$ (s, 9H), 2.84–2.31 (m, 2H), 3.20 (s, 3H), 3.24 (s, 3H), 4.99–5.08 (m, 2H), 7.20–7.33 ppm (m, 5H); ^{13}C NMR (126 MHz, $CDCl_3$): $\delta=28.2$, 30.4, 38.5, 41.2, 51.4, 80.0, 113.4, 127.1, 128.6, 129.2, 129.5, 135.6, 155.3, 173.6 ppm; LC-IT-TOF/MS: m/z calcd for $C_{17}H_{24}N_4O_3$: 333.1848 $[M+H]^+$; found: 333.1896.

(*S*)-Benzyl {1-[2-Cyano-1-methyl-2-(3-phenylpropyl)hydrazinyl]-1-oxo-3-phenylpropan-2-yl}carbamate (3d): Prepared according to the general procedure using **18d** (112 mg, 0.25 mmol), sodium acetate (82 mg, 1.0 mmol), and cyanogen bromide (106 mg, 1.0 mmol) in anhydrous methanol (10 mL) to afford **3d** (82 mg, 72%) as a white solid. ^{1}H NMR (500 MHz, $CDCl_3$): $\delta=2.09$–2.11 (m, 2H), 2.65–2.90 (m, 4H), 3.08–3.16 (m, 2H), 3.19 (s, 3H), 3.32–3.37 (m, 1H), 3.44–3.49 (m, 1H), 4.98–5.15 (m, 2H), 5.32 (br s, 1H), 7.14–7.34 ppm (m, 15H); ^{13}C NMR (126 MHz, $CDCl_3$): $\delta=28.1$, 31.5, 32.5, 38.4, 52.2, 53.6, 67.0, 112.3, 126.4, 127.3, 127.9, 128.2, 128.3, 128.5, 128.7, 128.8, 129.2, 129.5, 135.4, 139.9, 155.8, 173.4 ppm; LC-IT-TOF/MS: m/z calcd for $C_{28}H_{30}N_4O_3$: 471.2318 $[M+H]^+$; found: 471.2365.

Mu-CO-Phe-hPh-al (4): $LiAlH_4$ (57 mg, 1.5 mmol) was added with vigorous stirring to a solution of **22** (480 mg, 1 mmol) in anhydrous THF (25 mL) at 0°C. The mixture was stirred for an additional 20 min at 0°C, whereupon cold water was carefully added until effervescence ceased. Cold HCl (1M) was added to break up the gelatinous emulsion until pH 6–7 was reached. The mixture was diluted with H_2O (50 mL) and extracted with EtOAc (3×25 mL). The combined organic extracts were washed with saturated aqueous $NaHCO_3$ and brine, dried over Na_2SO_4, filtered, and concentrated in vacuo. Purification by flash column chromatography (silica gel) using 50 to 75% EtOAc in hexanes gave **4** (350 mg, 73%) as a white solid. ^{1}H NMR (500 MHz, $CDCl_3$): $\delta=1.79$–1.85 (m, 1H), 2.10–2.13 (m, 1H), 2.50–2.60 (m, 2H), 3.11–3.13 (m, 2H), 3.25–3.36 (m, 4H), 3.57–3.62 (m, 4H), 4.25–4.31 (m, 1H), 4.76 (dd, $J=10.0$, 15.0 Hz, 1H), 5.60 (t, $J=10.0$ Hz, 1H), 7.11–7.42 (m, 10H), 9.31 ppm (s, 1H); ^{13}C NMR (126 MHz, $CDCl_3$): $\delta=30.1$, 31.2, 38.7, 43.9, 55.7, 58.3, 66.2, 126.3, 127.0, 128.3, 128.48, 128.52, 129.25, 129.31, 136.7, 140.3, 157.1, 172.9, 199.1 ppm; LC-IT-TOF/MS: m/z calcd for $C_{24}H_{29}N_3O_4$: 424.2158; $[M+H]^+$; found: 424.2164.

(*S*)-4-Ethynylbenzyl 1-(2-Benzyl-2-cyano-1-methylhydrazinyl)-1-oxo-3-phenylpropan-2-ylcarbamate (5): Prepared according to the general procedure using **26** (88 mg, 0.2 mmol), anhydrous sodium acetate (66 mg, 0.8 mmol), and cyanogen bromide (85 mg, 0.8 mmol) in anhydrous MeOH (5 mL) to afford **5** (81 mg, 87%) as a white solid. ^{1}H NMR (500 MHz, $CDCl_3$): $\delta=2.83$–2.87 (m, 2H), 3.09 (s, 1H), 3.12 (s, 3H), 4.52 (dd, $J=10.0$, 15.0 Hz, 2H), 5.02–5.08 (m, 4H), 5.38 (d, $J=10.0$ Hz, 1H), 7.13–7.48 ppm (m, 14H); ^{13}C NMR (126 MHz, $CDCl_3$): $\delta=32.3$, 38.4, 53.5, 59.0, 66.4, 77.6, 83.2, 112.2, 127.3, 127.7, 128.7, 129.2, 129.3, 129.5, 129.7, 129.8, 130.2, 131.2, 132.2, 135.4, 136.8, 155.8, 173.4 ppm; LC-IT-TOF/MS: m/z calcd for $C_{28}H_{26}N_4O_3$: 467.2005 $[M+H]^+$; found: 467.2104.

4-Ethynylbenzyl [(*S*)-1-{[(*S*)-4-diazo-3-oxobutan-2-yl]amino}-1-oxo-3-phenylpropan-2-yl]carbamate (6b): Prepared according to the general procedure using **29b** (0.39 g, 1.0 mmol), NMM (0.15 mL, 1.2 mmol), ISCF (0.17 mL, 1.2 mmol), and the diazomethane-ether solution. Purification by flash column chromatography (silica gel) using 25 to 50% EtOAc in hexanes gave **6b** (0.37 g, 89%) as a white solid. ^{1}H NMR (500 MHz, $[D_6]$DMSO): $\delta=1.22$ (d, $J=10.0$ Hz, 3H), 2.78 (dd, $J=5.0$, 105.0 Hz, 1H), 3.03 (dd, $J=5.0$, 10.0 Hz, 1H), 4.18 (s, 1H), 4.26–4.32 (m, 2H), 4.96 (s, 2H), 5.80 (s, 1H), 7.16–7.32 (m, 6H), 7.44 (d, $J=5.0$ Hz, 2H), 7.62 (d, $J=10.0$ Hz, 1H), 8.45 ppm (d, $J=5.0$ Hz, 1H); ^{13}C NMR (126 MHz, $[D_6]$DMSO): $\delta=16.9$, 37.4, 52.2, 55.9, 64.7, 80.8, 83.2, 120.9, 126.2, 127.5, 128.0, 129.3, 131.6, 137.9, 138.0, 155.7, 171.3, 195.1 ppm; LC-IT-TOF/MS: m/z calcd for $C_{23}H_{22}N_4O_4$: 419.1641 $[M+H]^+$; found: 419.1760.

Enzyme assays: Cruzain and rhodesain were assayed in freshly prepared 100 mM acetate buffer (pH 5.5), containing 5 mM dithiothreitol (DTT) and 0.001% Triton X-100. Reagents (25 μL; cruzain, or rhodesain at 4 nM final concentration) were added to a 384-well black plate (Greiner, Germany) that contained the test compound (1 μL; concentration ranging from 10 μM to 10 pM). The enzyme–compound mixture was incubated for 5 min at RT, then substrate Z-FR-AMC (25 μL; Bachem, 10 μM final concentration, in the same buffer solution as above) was added to initiate the reaction. The rate of increase in fluorescence (resulting from the proteolytic cleavage of the substrate leading to the release of fluorogenic AMC) was monitored with an automated microtiter plate spectrofluorimeter (BioTek Synergy 4 Fluorescence Plate Reader) with fluorescence readout setting of excitation at 355 nm and emission at 460 nm. Control experiments were performed by using enzyme alone, enzyme with DMSO vehicle, and enzyme in the presence of the previously known, highly effective irreversible inhibitors K11002, K11777, and Z-Phe-Ala-CHN_2 (**6a**). IC_{50} values were determined by sigmoid dose-response curve fitting with GraphPad Prism software using inhibitor concentrations in the linear portion of a plot of inhibition versus log[I] (seven concentrations tested with at least two in the linear range). Data are given as the mean values of at least two independent assays.

***Trypanosoma brucei* assay**: The bloodstream forms of *T. brucei* were grown at 37°C and 5% CO_2 in HMI-9 medium supplemented with 20% heat-inactivated fetal bovine serum (FBS). Procyclic forms YTAT 1.1 were grown at 28°C and 5% CO_2 in Cunningham's medium supplemented with 15% heat-inactivated fetal bovine serum (FBS). Trypanosomes number and percentage viability were determined in 96-well plate format using the Guava ViaCount assay with a Guava PCA-96 system (Guava Technologies, USA) following the manufacturer's instructions. Briefly, trypanosomes were harvested in the exponential growth phase and diluted to a concentration of 1×10^5 cells/mL in complete growth medium. For larger screens, the diluted trypanosomes were aliquoted (200 μL) in sterile 96-well flat white opaque culture plates (Greiner, Germany) using a Sciclone ALH 3000 Liquid Handling Workstation (Caliper Life Sciences, USA). For small-scale screens, diluted trypanosomes were dispensed manually using a multichannel pipette (BrandTech, USA). Positive and negative control experiments were performed by using K11002, K11777, Z-Phe-Ala-CHN_2 (**6a**) and 1.25% DMSO, respectively. After 24 h incubation with compounds, the cell density and viability were evaluated by using the ViaCount assay on a Guava PCA-96 system. ED_{50} values were

calculated by sigmoid curve fitting with GraphPad Prism 5.0 software (San Diego, USA). All data were collected in duplicate.

In situ proteomic profiling: *T. brucei* parasites were plated into 6-well plates (PCF, 2 mL at ca. 1×10^7 cells/mL) or 25 mL cell culture flasks (BSF, 10 mL at ca. 2×10^6 cells/mL), and incubated with the probe for 2 h at culture temperature with or without competing inhibitors, **3b** or Z-Phe-Ala-CHN_2 (**6a**). All compounds were solubilized in DMSO. To avoid adverse effects on parasite growth, the final DMSO concentration in the assay never exceeded 1.25% in cultivation medium. After incubation, the parasite cells were pelleted at 2000 rpm for 10 min, washed twice with PBS and resuspended in PBS (100 μL). Cells were homogenized by sonication and diluted to approximately 1 mg mL^{-1} with PBS. To initiate the click chemistry reaction, 20 μL of freshly premixed solution containing rhodamine-azide[30] (100 μM final concentration), TCEP (1 mM final concentration), TBTA (100 μM final concentration), and $CuSO_4$ (1 mM final concentration) was added. The reaction was incubated at 10°C for 4 h with gentle mixing. The reaction was terminated by addition of prechilled acetone (0.5 mL). The resulting solution was then placed at −20°C for 30 min, followed by centrifugation (13000 rpm × 10 min) at 4°C. The supernatant was discarded and the precipitated protein pellets were washed with prechilled methanol (2×200 μL), air-dried for 10 min, resuspended in 1 × standard reducing SDS-loading buffer (25 μL) then heated for 10 min at 95°C. Finally, the protein sample (ca. 20 μg/lane) was loaded onto 12% SDS-PAGE gel, separated, and analyzed by in-gel fluorescence scanning with a Typhoon 9410 Variable Mode Imager scanner (GE Amersham).

Affinity pull-down and LC/MS-MS experiments: For proteomic experiments, BSF and PCF trypanosomes (ca. 2×10^9 cells, ca. 5 mg each), labeled in Cunningham's media (1×10^7 cells/mL) with **5** (1 μM), **6b** (10 μM) or DMSO (negative control), were harvested, washed, and homogenized in PBS. CuAAC reagents were added at the same concentrations as described above, except that biotin-azide[30] was substituted for rhodamine-azide. Acetone-precipitated, methanol-washed protein pellets were solubilized in PBS containing 0.1% (w/v) SDS by brief sonication. Insoluble materials were precipitated by centrifugation (13,000 g × 10 min) at 4°C. The supernatants were then incubated with gentle shaking at 4°C overnight with Neutravidin agarose beads (50 μL mg^{-1} protein, Prod #29204, Thermo Scientific, USA), which had been prewashed twice with PBS. After centrifugation, the bead/complexes were washed extensively eight times with 1% (w/v) SDS in PBS, three times with PBS, and twice with 250 mM ammonium bicarbonate (ABC). Elution of bound proteins from beads was then performed twice using boiling buffer (200 mM Tris, pH 6.8, 400 mM DTT, 8% (w/v) SDS), then pooled. Protein samples were concentrated using an YM-10 Centricon spin column (Millipore, USA). Following SDS-PAGE separation, protein bands were visualized by Coomassie blue staining. Gel lanes corresponding to both DMSO- and probe-treated samples were then each cut into several slices. Subsequent trypsin digestion (using In-Gel Trypsin Digestion Kit, Pierce Co., USA) and peptide extraction (with 50% acetonitrile and 1% formic acid) generated the corresponding LCMS samples for each pull-down experiment. All samples were dried in vacuo and stored at −20°C prior to LCMS analysis. Each LCMS sample was resuspended in 0.1% formic acid for mass spectrometry analysis as previously described.[40] Briefly, peptides were separated and analyzed with a Shimadzu UFLC system (Shimadzu, Kyoto, Japan) coupled to an LTQ-FT Ultra (Thermo Electron, Germany). Mobile phase A (0.1% formic acid in H_2O) and mobile phase B (0.1% formic acid in acetonitrile) were used to establish the 60 min gradient, which was comprised of 45 min of 5–35% B, 8 min of 35–50% B, and 2 min of 80% B followed by re-equilibrating at 5% B for 5 min. Peptides were then analyzed with an LTQ-FT with an ADVANCE CaptiveSpray Source (Michrom BioResources, USA) at an electrospray potential of 1.5 kV. A gas flow of 2 L min^{-1}, ion transfer tube temperature of 180°C and collision gas pressure of 0.85 mTorr were used. The LTQ-FT was set to perform data acquisition in the positive ion mode as previously described, except that an m/z range of 350–1600 was used in the full MS scan.[41] The raw data were converted into mgf format as previously described.[41] The database (76708 sequences, 33362815 residues) used for Mascot search was a concatenated *T. brucei* protein database. The database search was performed by using an in-house Mascot server (version 2.2.07, Matrix Science, UK) with MS tolerance of 10 ppm and MS/MS tolerance of 0.8 Da. Two missed cleavage sites of trypsin were allowed. Carbamidomethylation (C) was set as a fixed modification, and oxidation (M) and phosphorylation (S, T and Y) were set as variable modifications.

Pull-down and western blotting analysis: Pull-down samples from in situ labeling with **5** (1 μM) or **6b** (10 μM) were separated on 12% SDS-PAGE gels together with a pull-down sample from DMSO-treatment (negative control). After SDS-PAGE gel separation, proteins were then transferred to a PVDF membrane and subsequently blocked with 3% (w/v) BSA/PBST overnight at 4°C. Membranes were incubated for 1 h at RT with the respective antibodies (anti-cathepsin L for HepG2; anti-rhodesain or anti-TbcatB for *T. brucei*), and washed with PBST (3×15 min with gentle agitation), then incubated with an anti-mouse-IgG conjugated secondary antibody in the blocking buffer mentioned above. After washing with PBST (3×15 min with gentle agitation), the SuperSignal West Pico kit (Pierce) was used to develop the blot.

Fluorescence microscopy: For drug uptake analysis, trypanosomes (1×10^5 cells/mL for both forms) were incubated in growth medium containing different concentrations of **5** or **6b** at culture temperature and 5% CO_2 for 2 h. Medium containing 1% DMSO was used as a negative control. The parasites were then washed twice with PBS, fixed with 4% paraformaldehyde in PBS for 15 min at RT, washed with PBS (2×5 min with gentle agitation), and then sedimented to poly-L-lysine-coated coverslips. Fixed cells were permeabilized with 0.25% Triton-X 100 in PBS for 15 min at RT, and washed with PBS (2×5 min with gentle agitation). The cells were blocked with 3% BSA in PBS for 30 min at RT, and washed with PBS (2×5 min with gentle agitation). The cells were then treated with a freshly pre-mixed click chemistry reaction solution (rhodamine-azide (10 μM final concentration from a 10 mM stock solution in DMSO), TCEP (1 mM final concentration from a 50 mM freshly prepared stock solution in deionized water), TBTA (100 μM final concentration from a 10 mM stock solution in DMSO), and $CuSO_4$ (1 mM final concentration from a 100 mM freshly prepared stock solution in deionized water)) in PBS for 1 h at RT. The cells were washed with PBS (5 min with gentle agitation), and cold methanol (5 min with gentle agitation), followed by 1% Tween-20 and 0.5 mM of EDTA in PBS (3×2 min with gentle agitation), and with PBS (2×5 min with gentle agitation). The cells were then incubated in PBS containing 2 μg mL^{-1} DAPI for 15 min at RT to stain the kinetoplast and nuclear DNA, and washed with PBS (2×5 min with gentle agitation) and finally washed with deionized water (1×5 min with gentle agitation) before mounting onto the Fluoromount G (Emsdiasum, USA). For immunofluorescence (IF) analysis, cells were then incubated for 1h in PBS with rabbit anti-rhodesain (1:1000) and washed with PBS (3×5 min with gentle agitation), then labeled with FITC-conjugated goat anti-rabbit IgG antibody (1:500) and finally washed with PBS (3×5 min with gentle agitation) before mounting. Confocal images were taken with a Leica TCS SP5X Confocal Microscope System equipped with Leica HCX PL APO 100×/1.40 oil objective, 405 nm Diode laser, White laser (470 to 670 nm, with 1 nm increments, with 8 channels AOTF for simultaneous control of eight laser lines, each excitation wavelength provides 1.5 mV, PMT detector range from 420 to 700 nm) was used to measure the steady-state fluorescence. DAPI, FITC, and rhodamine were excited with a krypton/argon laser at 405, 488, and 554 nm, respectively, and the emission was collected through 420–470, 500–550, and 565–650 nm filters, respectively. Images were processed with Leica Application Suite Advanced Fluorescence (LAS AF).

In situ proteome profiling and fluorescence microscopy in HepG2 mammalian cells: Our previous published procedures were followed.[30,42] Briefly, cells were grown to 80–90% confluence in 24-well plates, and medium was removed, washed twice with cold PBS, then treated with 0.5 mL of DMEM-containing probe for 2 h (the final DMSO concentration in the assay never exceeded 1% in cultivation medium) as mentioned above. After incubation, the growth medium was aspirated and cells were washed twice with PBS to remove the excess probe, trypsined, and pelleted at 1,000 rpm for 10 min, washed twice with PBS, and resuspended in PBS (100 μL). Cells were homogenized by sonication, diluted to approximately 1 mg mL^{-1} with PBS, then submitted to click chemistry, SDS-PAGE gel analysis, and in-gel fluorescence scanning (Figure S3 in

the Supporting Information). For cellular imaging, cells were grown to approximately 50% confluence in 24-well plates containing sterile glass coverslips, and medium was removed, washed twice with cold PBS, then treated with 0.5 mL DMEM-containing probe for 2 h. After incubation, the growth medium was aspirated and cells were washed twice with PBS. Cells were fixed, permeabilized, and blocked, then submitted to click chemistry, washing, staining (for IF, using mouse anti-cathepsin L; 1:100), mounted, and imaged (Figure S6 in the Supporting Information).

Acknowledgements

We gratefully acknowledge generous gifts of recombinant enzymes (cruzain and rhodesain) and antibodies (anti-rhodesain and anti-TbCatB) from Dr. Conor R. Caffrey and Professor James H. McKerrow (University of California, San Francisco). We thank Professor Siu Kwan Sze (Nanyang Technological University, Singapore) for his continuous support for LC-MS/MS experiments. This work was supported by the Ministry of Education (R-143–000–394–112), the Agency for Science, Technology and Research (A*Star) (R143–000–391–305), and the Competitive Research Program (NRF-G-CRP 2007–04) of the National Research Foundation (NRF). This work was also supported in part by funding from the Singapore National Research Foundation, awarded to C. Y. H as a research fellow.

[1] P. J. Hotez, D. H. Molyneux, A. Fenwick, J. Kumaresan, S. E. Sachs, J. D. Sacha, L. Savioli, *N. Engl. J. Med.* **2007**, *357*, 1018–1027.
[2] C. Young, P. Losikoff, A. Chawla, L. Glasser, E. Forman, *Transfusion* **2007**, *47*, 540–544.
[3] A. R. Renslo, J. H. McKerrow, *Nat. Chem. Biol.* **2006**, *2*, 701–710.
[4] A. Cavalli, M. L. Bolognesi, *J. Med. Chem.* **2009**, *52*, 7339–7459.
[5] S. C. Barr, K. L. Warner, B. G. Kornreic, J. Piscitelli, A. Wolfe, L. Benet, J. H. McKerrow, *Antimicrob. Agents Chemother.* **2005**, *49*, 5160–5161.
[6] Z. B. Mackey, T. C. O'Brien, D. C. Greenbaum, R. B. Blank, J. H. McKerrow, *J. Biol. Chem.* **2004**, *279*, 48426–48433.
[7] a) M. Sajid, J. H. McKerrow, *Mol. Biochem. Parasitol.* **2002**, *120*, 1–21; b) P. S. Doyle, M. Sajid, T. O'Brien, K. DuBois, J. C. Engel, Z. B. Mackey, S. Reed, *Curr. Pharm. Des.* **2008**, *14*, 889–900.
[8] a) J. C. Engel, P. S. Doyle, I. Hsieh, J. H. McKerrow, *J. Exp. Med.* **1998**, *188*, 725–734; b) P. S. Doyle, Y. M. Zhou, J. C. Engel, J. H. McKerrow, *Antimicrob. Agents Chemother.* **2007**, *51*, 3932–3939.
[9] a) C. R. Caffrey, S. Scory, D. Steverding, *Curr. Drug Targets* **2000**, *1*, 155–162; b) O. V. Nikolskaia, A. P. de A Lima, Y. V. Kim, J. D. Lonsdale-Eccles, T. Fukuma, J. Scharfstein, D. J. Grab, *J. Clin. Invest.* **2006**, *116*, 2739–2747.
[10] P.-Y. Yang, M. Wang, C. Y. He, S. Q. Yao, *Chem. Commun.* **2012**, *48*, 835–837.
[11] a) S. Scory, Y. D. Stierhof, C. R. Caffrey, D. Steverding, *Kintoplastid Bio. Dis.* **2007**, *6*, 2; b) S. Scory, C. R. Caffrey, Y. D. Stierhof, A. Ruppel, D. Steverding, *Exp. Parasitol.* **1999**, *91*, 327–333.
[12] a) D. Brak, P. S. Doyle, J. H. McKerrow, J. A. Ellman, *J. Am. Chem. Soc.* **2008**, *130*, 6404–6410; b) K. Brak, I. D. Kerr, K. T. Barrett, N. Fuchi, M. Debnath, K. Ang, J. C. Engel, J. H. McKerrow, P. S. Doyle, L. S. Brinen, J. A. Ellman, *J. Med. Chem.* **2010**, *53*, 1763–1773; c) J. H. McKerrow, J. C. Engel, C. R. Caffrey, *Bioorg. Med. Chem.* **1999**, *7*, 639–644.
[13] J.-P. Falgueyret, W. C. Black, W. Cromlish, S. Desmarais, S. Lamontagne, C. Mellon, D. Riendeau, S. Rodan, P. Tawa, G. Wesolowski, K. E. Bass, S. Venkatraman, M. D. Percival, *Anal. Biochem.* **2004**, *335*, 218–227.
[14] a) M. Bogyo, J. S. McMaster, M. Gaczynska, D. Tortorella, A. L. Goldberg, H. Ploegh, *Proc. Natl. Acad. Sci. USA* **1997**, *94*, 6629–6634; b) T. Mc Cormack, W. Baumeister, L. Grenier, C. Moomaw, L. Plamondon, B. Pramanik, C. Slaughter, F. Soucy, R. Stein, F. Zuhl, L. Dick, *J. Biol. Chem.* **1997**, *272*, 26103–26109.
[15] B. J. Lee, A. Singh, P. Chiang, S. J. Kemp, E. A. Goldman, M. I. Weinhouse, G. P. Vlasuk, P. J. Rosenthal, *Antimicrob. Agents Chemother.* **2003**, *47*, 3810–3814.
[16] R. Löser, M. Frizler, K. Schilling, M. Gütschow, *Angew. Chem.* **2008**, *120*, 4403–4406; *Angew. Chem. Int. Ed.* **2008**, *47*, 4331–4334.
[17] a) M. Frizler, F. Lohr, N. Furtmann, J. Kläs, M. Gütschow, *J. Med. Chem.* **2011**, *54*, 396–400; b) M. Frizler, F. Lohr, M. Lülsdorff, M. Gütschow, *Chem. Eur. J.* **2011**, *17*, 11419–11423.
[18] R. Löser, J. Gut, P. J. Rosenthal, M. Frizler, M. Gütschow, K. T. Andrews, *Bioorg. Med. Chem. Lett.* **2010**, *20*, 252–255.
[19] Y. Loh, H. Shi, M. Hu, S. Q. Yao, *Chem. Commun.* **2010**, *46*, 8407–8409.
[20] J. Singh, R. U. Petter, T. A. Baillie, A. Whitty, *Nat. Rev. Drug Discovery* **2011**, *10*, 307–317.
[21] J. A. Frearson, P. G. Wyatt, I. H. Gilbert, A. H. Fairlamb, *Trends Parasitol.* **2007**, *23*, 589–597.
[22] a) M. J. Evans, B. F. Cravatt, *Chem. Rev.* **2006**, *106*, 3279–3301; b) M. Fonović, M. Bogyo, *Expert Rev. Proteomics* **2008**, *5*, 721–730; c) M. Uttamchandani, J. Li, H. Sun, S. Q. Yao, *ChemBioChem* **2008**, *9*, 667–675; d) T. Bottcher, M. Pitscheider, S. A. Sieber, *Angew. Chem.* **2010**, *122*, 2740–2759; *Angew. Chem. Int. Ed.* **2010**, *49*, 2680–2698; e) W. P. Heal, T. H. T. Dang, E. W. Tate, *Chem. Soc. Rev.* **2011**, *40*, 246–257.
[23] a) L. I. Willems, W. A. van der Linden, N. Li, K.-Y. Li, N. Liu, S. Hoogendoorn, G. A. van der Marel, B. I. Florea, H. S. Overkleeft, *Acc. Chem. Res.* **2011**, *44*, 718–729; b) E. M. Sletten, C. R. Bertozzi, *Angew. Chem.* **2009**, *121*, 7108–7133; *Angew. Chem. Int. Ed.* **2009**, *48*, 6974–6998; c) K. A. Kalesh, H. Shi, J. Ge, S. Q. Yao, *Org. Biomol. Chem.* **2010**, *8*, 1749–1762.
[24] Z. Anamarija, *Curr. Med. Chem.* **2005**, *12*, 589–597.■■author name changed to match records, ok?■■
[25] a) L. S. Brinen, E. Hansell, J. Cheng, W. R. Roush, J. H. McKerrow, R. J. Fletterick, *Structure* **2000**, *8*, 831–840; b) I. D. Kerr, C. J. Farady, R. Marion, M. Richert, M. Sajid, K. C. Pandey, C. R. Caffrey, J. Legac, E. Hansell, J. H. McKerrow, C. S. Craik, P. J. Rosenthal, L. S. Brinen, *J. Biol. Chem.* **2009**, *284*, 25697–25703; c) I. D. Kerr, P. Wu, R. Marion-Tsukamaki, Z. B. Mackey, L. S. Brinen, *PLoS Negl. Trop. Dis.* **2010**, *4*, e701.
[26] a) C. R. Caffrey, E. Hansell, K. D. Lucas, L. S. Brinen, A. Alvarez Hernandez, J. Cheng, S. L. Gwaltney II, W. R. Roush, Y.-D. Stierhof, M. Bogyo, D. Steverding, J. H. McKerrow, *Mol. Biochem. Parasitol.* **2001**, *118*, 61–73; b) P. Jaishankar, E. Hansell, D.-M. Zhao, P. S. Doyle, J. H. McKerrow, A. R. Renslo, *Bioorg. Med. Chem. Lett.* **2008**, *18*, 624–628.
[27] R. Löser, K. Schilling, E. Dimmig, M. Gütschow, *J. Med. Chem.* **2005**, *48*, 7688–7707.
[28] M. H. Abdulla, T. O'Brien, Z. B. Mackey, M. Sajid, D. J. Grab, J. H. McKerrow, *PLoS Negl. Trop. Dis.* **2008**, *2*, e298.
[29] C. R. Caffrey, D. Steverding, *Mol. Biochem. Parasitol.* **2009**, *167*, 12–19.
[30] a) P.-Y. Yang, K. Liu, M. H. Ngai, M. J. Lear, M. R. Wenk, S. Q. Yao, *J. Am. Chem. Soc.* **2010**, *132*, 656–666; b) P.-Y. Yang, K. Liu, C.-J. Zhang, G. Y. J. Chen, Y. Shen, M. H. Ngai, M. J. Lear, S. Q. Yao, *Chem. Asian J.* **2011**, *6*, 2762–2775; c) H. Shi, X.-M. Cheng, S. K. Sze, S. Q. Yao, *Chem. Commun.* **2011**, *47*, 11306–11308; d) H, Wu, J. Ge, P.-Y. Yang, J. Wang, M. Uttamchandani, S. Q. Yao, *J. Am. Chem. Soc.* **2011**, *133*, 1946–1954; e) K. Liu, P.-Y. Yang, Z. Na, S. Q. Yao, *Angew. Chem.* **2011**, *123*, 6908–6913; *Angew. Chem. Int. Ed.* **2011**, *50*, 6776–6781; f) H. Shi, M. Uttamchandani, S. Q. Yao, *Chem. Asian J.* **2011**, *6*, 2803–2815; g) K. Liu, H. Shi, H. Xiao, A. G. L. Chong, X. Bi, Y. T. Chang, K. Tan, R. Y. Yada, S. Q. Yao, *Angew. Chem.* **2009**, *121*, 8443–8447; *Angew. Chem. Int. Ed.* **2009**, *48*, 8293–8297.
[31] T. C. O'Brien, Z. B. Mackey, R. D. Fetter, Y. Choe, A. J. O'Donoghue, M. Zhou, C. S. Craik, C. R. Caffrey, J. H. McKerrow, *J. Biol. Chem.* **2008**, *283*, 28934–28943.
[32] a) S. Alsford, D. J. Turner, S. O. Obado, A. Sanchez-Flores, L. Glover, M. Berriman, C. Hertz-Fowler, D. Horn, *Genome Res.* **2011**, *21*, 915–924; b) J. Rubotham, K. Woods, J. A. Garcia-Salcedo, E.

Pays, D. P. Nolan, *J. Biol. Chem.* **2005**, *280*, 10410–10418; c) C. X. Moss, G. D. Westrop, L. Juliano, G. H. Coombs, J. C. Mottram, *FEBS Lett.* **2007**, *581*, 5635–5639; d) L. Huang, M. Shen, I. Chernushevich, A. L. Burlingame, C. C. Wang, C. D. Robertson, *Mol. Biochem. Parasitol.* **1999**, *102*, 211–223.

[33] a) G. I. Lepesheva, R. D. Ott, T. Y. Hargrove, Y. Y. Kleshchenko, I. Schuster, W. D. Nes, G. C. Hill, F. Villalta, M. R. Waterman, *Chem. Biol.* **2007**, *14*, 1283–1293; b) G. I. Lepesheva, H.-W. Park, T. Y. Hargrove, B. Vanhollebeke, Z. Wawrzak, J. M. Harp, M. Sundaramoorthy, W. David Nes, E. Pays, M. Chaudhuri, F. Villalta, M. R. Waterman, *J. Biol. Chem.* **2010**, *285*, 1773–1780; c) C. K. Chen, S. S. Leung, C. Guilbert, M. P. Jacobson, J. H. McKerrow, L. M. Podust, *PLoS Negl. Trop. Dis.* **2010**, *4*, e651.

[34] T. K. Smith, P. Bütikofer, *Mol. Biochem. Parasitol.* **2010**, *172*, 66–79.

[35] M. Bonhivers, S. Nowacki, N. Landrein, D. R. Robinson, *PLoS Biol.* **2008**, *6*, e105.

[36] I. Hunger-Glaser, R. Brun, M. Linder, T. Seebeck, *Mol. Biochem. Parasitol.* **1999**, *100*, 53–59.

[37] a) T. Nomura, N. Katunuma, *J. Med. Invest.* **2005**, *52*, 1–9; b) J. M. Lankelma, D. M. Voorend, T. Barwari, J. Koetsveld, A. H. Van der Spek, A. P. De Porto, G. Van Rooijen, C. J. Van Noorden, *Life Sci.* **2010**, *86*, 225–233.

[38] a) K. Chandran, N. J. Sullivan, U. Felbor, S. P. Whelan, J. M. Cunningham, *Science* **2005**, *308*, 1643–1645; b) C. T. Pager, R. E. Dutch, *J. Virol.* **2005**, *79*, 12714–12720; c) G. Simmons, D. N. Gosalia, A. J. Rennekamp, J. D. Reeves, S. L. Diamond, P. Bates, *Proc. Natl. Acad. Sci. USA* **2005**, *102*, 11876–11881.

[39] a) H. H. Otto, T. Schirmeister, *Chem. Rev.* **1997**, *97*, 133–171; b) J. C. Powers, J. L. Asgian, Ö. D. Ekici, K. E. James, *Chem. Rev.* **2002**, *102*, 4639–4750.

[40] P. Hao, T. Guo, X. Li, S. S. Adav, J. Yang, M. Wei, S. K. Sze, *J. Proteome Res.* **2010**, *9*, 3520–3526.

[41] C. S. Gan, T. Guo, H. Zhang, S. K. Lim, S. K. Sze, *J. Proteome Res.* **2008**, *7*, 4869–4877.

[42] a) H. Shi, C.-J. Zhang, G. Y. J. Chen, S. Q. Yao, *J. Am. Chem. Soc.* **2012**, *134*, 3001–3014; b) C.-J. Zhang, L. Li, G. Y. J. Chen, Q.-H. Xu, S. Q. Yao, *Org. Lett.* **2011**, *13*, 4160–4163; c) M. Hu, L. Li, H. Wu, Y. Su, P.-Y. Yang, M. Uttamchandani, Q.-H. Xu, S. Q. Yao, *J. Am. Chem. Soc.* **2011**, *133*, 12009–12020; d) J. Li, S. Q. Yao, *Org. Lett.* **2009**, *11*, 405–408.

Received: October 21, 2011
Published online: ■■ ■■, 2012

